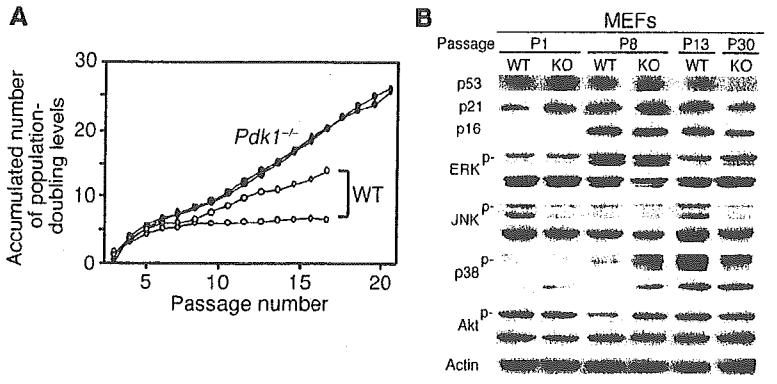


**Figure 8**
Outgrowing *Pkd1*$^{-/-}$ MEFs. (**A**) The 3T3-type culture of MEFs from *Pkd1*$^{-/-}$ and wild-type mice. (**B**) Signaling pathways related to proliferation or apoptosis in *Pkd1*$^{-/-}$ MEFs. Expression of signal transducers and cell cycle regulators was analyzed using Western blot. Actin was used as a loading control for protein. Data presented are 1 representative of 4 independent experiments.

cytoskeletal organization. However, the localization and intensity of both E-cadherin and β-catenin in some cyst epithelial cells were similar to those in normal renal tubular cells at the intermediate stage of cystogenesis (data not shown). These results indicate that the morphological change in cyst epithelial cells is not due to loss of tubular markers or to repression of cell adhesion molecules. As *Pkd1*$^{-/-}$ cyst epithelial cells cultured in collagen gel sometimes made tubules in the gel (data not shown), outgrowing *Pkd1*$^{-/-}$ cyst epithelial cells retain some functions of renal tubular epithelial cells. Further studies will be done to elucidate the cause of the morphological change and the dedifferentiation (loss of tubular markers) of cyst epithelial cells initiated by deficiency in the *Pkd1* gene.

*Apoptosis on normal (LZ*$^{+}$*) cyst epithelial cells.* Apoptosis has been frequently observed in non-dilated and cystic tubuli and glomeruli in ADPKD kidneys, whereas it is extremely rare in normal kidneys (46). In addition, the increased rate of growth in cyst epithelial cells is accompanied by an increased rate of apoptosis in human ADPKD (26). Of note, our study showed that apoptotic cells were present mainly in cuboidal epithelial cells in *Pkd1*$^{-/-}$/LZ$^{+}$ kidneys. Electron microscopy revealed characteristic apoptotic features among cuboidal cyst epithelium, which was covered by flat cells. Apoptotic cells were lost from cyst epithelium and neighboring flat cells lined tubular lumina. These findings suggest net replacement of cuboidal LZ$^{+}$ epithelial cells by flat *Pkd1*$^{-/-}$ epithelial cells.

Expression of p-JNK increased in *Pkd1*$^{-/-}$/LZ$^{+}$ kidneys but not in *Pkd1*$^{-/-}$ kidneys. In contrast, Bcl-$X_L$ expression was decreased in *Pkd1*$^{-/-}$/LZ$^{+}$ kidneys but not in *Pkd1*$^{-/-}$ kidneys. Although p-Akt expression was significantly increased in both cuboidal and flat cyst epithelial cells, cuboidal cyst epithelial cells are more apoptotic than are flat cyst epithelial cells. The 3T3 cell cultures using *Pkd1*$^{-/-}$ MEFs also demonstrated that expression of p-JNK and p-p38 was increased in wild-type MEFs at the cell senescence stage (after passage 13). However, this expression did not increase in immortalized *Pkd1*$^{-/-}$ MEFs until passage 30. As polycystin-1 triggers activation of JNK but not that of p38 (47), flat *Pkd1*$^{-/-}$ epithelial cells and *Pkd1*$^{-/-}$ MEFs in the 3T3 culture escape apoptosis mediated by activation of JNK. These immortalized flat *Pkd1*$^{-/-}$ epithelial cells slowly spread to form large cysts.

*A model of cystogenesis.* We developed chimeric mice by aggregation of *Pkd1*$^{-/-}$ ES cells and *Pkd1*$^{+/+}$ morulae of LZ$^{+}$ ROSA26 mice. These mice are a unique mouse model for human ADPKD. In *Pkd1*$^{-/-}$/LZ$^{+}$ kidneys, sporadic *Pkd1*$^{-/-}$ epithelial cells deteriorated the entire tubular integrity by the proliferation of both *Pkd1*$^{-/-}$ and normal (LZ$^{+}$) epithelial cells at the early stage of cystogenesis (Figure 9). When tubular epithelial cells, including *Pkd1*$^{-/-}$ epithelial cells, receive stimulation, both *Pkd1*$^{-/-}$ and normal tubular epithelial cells proliferate to expand the tubular size. The *Pkd1*$^{-/-}$ tubular epithelial cells lack negative signals for proliferation by polycystin-1 and continue to proliferate. Although surrounding normal tubular epithelial cells also proliferate to retain both the round shape and diameter of the tubule, normal epithelial cells are gradually lost by JNK-mediated apoptosis at the intermediate stage. Some *Pkd1*$^{-/-}$ tubular epithelial cells change shape from cuboidal to flat (dedifferentiation), and the flat *Pkd1*$^{-/-}$ epithelial cells grow in an immortalized fashion to form large cysts in the kidney at the late stage of cystogenesis. As p53 expression and JNK activation were very low in flat *Pkd1*$^{-/-}$ cyst epithelial cells, polycystin-1 plays a role in the prevention of immortalized proliferation of renal tubular epithelial cells via p53 induction and JNK activation.

## Methods

*Generation of Pkd1*$^{-/-}$ *mice.* Murine *Pkd1* genomic clones were obtained by screening a 129/Sv mouse genomic library (14). R1 ES cells were transfected with linearized *Pkd1* neomycin-targeting vectors by electroporation and were subjected to positive and negative selection for 14 days using G418 and diphtheria toxin. Approximately 134 clones were examined using Southern blot, and homologous recombination was detected in 18 clones. One independent targeted ES clone was used to generate chimeric mice using the aggregation method (48). DNA from tail tissue of agouti pups

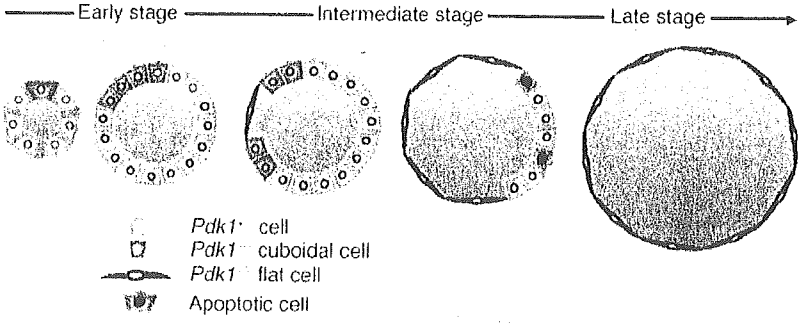


**Figure 9**
A model schema of the cystogenesis in ADPKD. The germline mutation of 1 allele of the *Pkd1* gene is present in all tubular epithelial cells.

obtained by mating chimeric mice with C57BL/6 mice (Japan SLC) was analyzed using Southern blot. Homozygous mutant pups were generated by intercrossing of heterozygous mutant mice. All procedures conformed to the Chiba University Resolution on Use of Animals in Research and were approved by the Institutional Animal Care and Use Committee of the Graduate School of Medicine, Chiba University (Chiba, Japan).

*Generation of Pkd1 ES cells and Pkd1 LZ chimeric mice.* One of the *Pkd1*-targeted ES clones was transfected by electroporation with linearized *Pkd1* hygromycin targeting vectors to generate *Pkd1* ES cells. Approximately 17 ES clones were examined by Southern blot, and 4 independent *Pkd1* ES clones were obtained. Those *Pkd1* ES cells were aggregated with morulae of ROSA26 mice with the exogenous *LacZ* gene (a gift from H. Koseki, RIKEN Research Center for Allergy and Immunology, Yokohama, Japan) to generate *Pkd1* /LZ chimeric mice.

*Southern blot.* Genotyping was done by digestion of genomic DNA (10 μg) with *Eco*RV, Southern transfer, and hybridization with a 1.3-kb DNA probe that was external to the targeting vector. The probe was labeled with digoxigenin (Roche Diagnostics) using PCR. The probe detected the wild-type allele as a 15.1-kb fragment and the mutant alleles as 7.7-kb and 8.3-kb fragments.

*Histology and immunohistochemistry.* Tissues were fixed in 10% phosphate-buffered formalin and were embedded in paraffin. Sections (3 μm thick) were stained with H&E according to standard protocols. For immunohistochemistry, after deparaffinization through a graded xylene and ethanol series, sections were washed in PBS (pH 7.4) and were treated for 15 minutes with 0.3% hydrogen peroxide in methanol. After blocking, sections were stained with the following antibodies: anti-p53, anti-p-EGFR (Santa Cruz Biotechnology Inc.), and anti-PCNA (Sigma-Aldrich). For immunofluorescence, frozen section were stained with YCC2 (anti-polycystin-2; a kind gift from Y. Cai, Yale University, New Haven, Connecticut, USA), anti-β-gal (Chemicon International Inc.), anti-Na-K ATPase (Upstate), anti-acetylated tubulin, anti-DBA, anti-lectin *Lotus tetragonolobus* (Sigma-Aldrich), anti-p-ERK, anti-p-Akt, or anti-p-JNK (Cell signaling Technology Inc.). Photomicrographs were obtained using a microscope (Carl Zeiss International).

*β gal staining of kidneys.* Kidneys were fixed for 30 minutes at 4°C in 2.7% formaldehyde, 0.02% NP-40, and 0.2% glutaraldehyde in PBS (pH 7.4) and were washed. Processing was carried out through a graded series of sucrose concentrations from 15% to 30% in PBS at 4°C for 5–12 hours for each step. Kidneys were then embedded in OCT (Tissue-Tek) and were frozen in 2-methyl-butane submerged in liquid nitrogen. Sections (3 μm thick) were then prepared, mounted on slides, and washed in PBS for 5 minutes, and were subsequently stained at 37°C overnight in X-gal solution (1 mg/ml X-gal in DMSO, 2 mM $MgCl_2$, 20 mM potassium ferricyanide, 20 mM potassium ferrocyanide, and 0.02 % NP-40 in PBS). Sections were counterstained with Nuclear Fast Red (Trevigen Inc.).

*Microdissection of nephron segments.* Nephrons were isolated from the kidneys of wild-type, *Pkd1* , and *Pkd1* /LZ mice at E17.5. Microdissection of tubules was done in PBS under a stereomicroscope (2).

*Western blot.* Kidneys were sonicated in Tris lysis buffer (20 mM Tris-HCl, 150 mM NaCl, 100 mM NaF, 1 mM EDTA, 1 mM sodium orthovanadate, 1 mM phenylmethylsulfonyl fluoride, 1.5 nM aprotinin, and 10 nM leupeptin). Proteins were separated by SDS-PAGE and were transferred to polyvinylidene difluoride membranes (Millipore). Membranes were blocked with nonfat dry milk (Yukijirushi) and were incubated with the following antibodies: anti-p53, anti-p21, anti-ERK, anti-Bcl-$X_L$, anti-Bax, anti-p16, anti-actin (Santa Cruz Biotechnology Inc.), anti-Akt, anti-p-Akt, anti-p-ERK, anti-p38, anti-p-p38 (Cell Signaling Technology Inc.), anti-JNK, anti-p-JNK (BD Biosciences Pharmingen), or anti-Bcl-2 (R&D Systems). The filters were washed with TBS/0.1% Triton-X, and immunoreactive bands were visualized by enhanced chemiluminescence.

*In vitro culture of microdissected tubules.* Microdissection of tubules was done in L-15 medium (Sigma-Aldrich) followed by culture at 37°C in 5% $CO_2$ in collagen gel (Neutral Solution, DMEM Culture Medium; Koken) in DMEM supplemented with 10% FCS (Sigma-Aldrich).

*TUNEL assay.* Animals were perfused with a solution of 4% paraformaldehyde in 0.1 M phosphate buffer (pH 7.4). Organs were dissected and were post-fixed overnight with 4% paraformaldehyde. The tissues were equilibrated with 20% sucrose and were cut into sections 3 μm in thickness on a cryostat. The TUNEL assay was carried as described with slight modification (49). The tailing reaction was carried out for 1 hour at 37°C in TdT buffer in the presence of dUTP-biotin (The Mebstain Apoptosis kit, Medical & Biological Laboratories). Signals were visualized using Avidin-Rohdamine (Vector Laboratories). Sections were counterstained with DAPI (Molecular Probes).

*Electron microscopy.* Specimens were fixed in formalin followed by 2% glutaraldehyde, were post-fixed with 1% osmium tetroxide, and were embedded in epoxy resin mixture. Ultrathin sections were mounted on grids, stained with uranyl acetate–lead citrate, and observed under a transmission electron microscope (Hitachi).

*Cell culture.* MEFs were established from *Pkd1* embryos (E13.5). Heads and livers were removed from embryos, and the remaining embryonic tissues were trypsinized at 37°C for 30 minutes. The disrupted tissues were plated in DMEM supplemented with 10% FCS (Sigma-Aldrich) and were cultured at 37°C in 5% $CO_2$. The 3T3-type serial MEF cultivation was done as described (38). Briefly, $3 \times 10^5$ cells were plated on a 6-cm well; 3 days later, the total number of cells was counted, and $3 \times 10^5$ cells were plated on a separate well. The cumulative increase in cell number was calculated according to the formula $\mathrm{Log}(N_f / N_i)/\mathrm{Log}2$, where $N_i$ is the initial number of cells plated and $N_f$ is the final number of cells counted after 3 days.

*Statistical analysis.* Data presented represents the mean ± SD of more than 3 independent experiments. Statistical analysis was performed using an unpaired Student's *t* test. *P* values of less than 0.05 were considered to be significant.

## Acknowledgments

We are grateful to H. Koseki and S. Somlo for discussions and to Y. Cai for providing YCC2 (anti-polycystin-2). We also thank L. Fujimura, H. Satake, K. Hanaoka, J. Usui, S. Horita, and H. Hazawa for skillful technical assistance; N. Kakinuma for secretarial services; and M. Ohara for language assistance. This work was supported in part by Grants-in-Aid from the Ministry of Education, Science, Technology, Sports and Culture of Japan, a grant from the Inamori Foundation (to T. Mochizuki), and a grant from Sankyo Foundation of Life Science (to T. Mochizuki).

Received for publication July 28, 2004, and accepted in revised form January 11, 2005.

Address correspondence to: Toshio Mochizuki, Department of Medicine II, Hokkaido University Graduate School of Medicine, Kita 15, Nishi 7, Kita-ku, Sapporo 060-8638, Japan. Phone: 81-11-716-1161; Fax: 81-11-706-7710; E-mail: mtoshi@med.hokudai.ac.jp.

1. Gabow, P.A. 1993. Autosomal dominant polycystic kidney disease. *N. Engl. J. Med.* **329**:332–342.
2. Baert, L. 1978. Hereditary polycystic kidney disease (adult form): a microdissection study of two cases at an early stage of the disease. *Kidney Int.* **13**:519–525.
3. Wilson, P.D. 2004. Polycystic kidney disease. *N. Engl. J. Med.* **350**:151–164.
4. The European Polycystic Kidney Disease Consortium. 1994. The polycystic kidney disease 1 gene encodes a 14 kb transcript and lies within a duplicated region on chromosome 16. The

European Polycystic Kidney Disease Consortium. *Cell* **77**:881–894.
5. Mochizuki, T., et al. 1996. PKD2, a gene for polycystic kidney disease that encodes an integral membrane protein. *Science.* **272**:1339–1342.
6. Warnick, T.J., et al. 1998. Somatic mutation in individual liver cysts supports a two-hit model of cystogenesis in autosomal dominant polycystic kidney disease. *Mol. Cell.* **2**:247–251.
7. Qian, F., Warnick, T.J., Onuchic, L.F., and Germino, G.G. 1996. The molecular basis of focal cyst formation in human autosomal dominant polycystic kidney disease type I. *Cell.* **87**:979–987.
8. Pei, Y., et al. 1999. Somatic PKD2 mutations in individual kidney and liver cysts support a "two-hit" model of cystogenesis in type 2 autosomal dominant polycystic kidney disease. *J. Am. Soc. Nephrol.* **10**:1524–1529.
9. Brasier, J.L., and Henske, E.P. 1997. Loss of the polycystic kidney disease (PKD1) region of chromosome 16p13 in renal cyst cells supports a loss-of-function model for cyst pathogenesis. *J. Clin. Invest.* **99**:194–199.
10. Torra, R., et al. 1999. A loss-of-function model for cystogenesis in human autosomal dominant polycystic kidney disease type 2. *Am. J. Hum. Genet.* **65**:345–352.
11. Lu, W., et al. 1999. Late onset of renal and hepatic cysts in Pkd1-targeted heterozygotes. *Nat Genet* **21**:160–161.
12. Wu, G., et al. 1998. Somatic inactivation of Pkd2 results in polycystic kidney disease. *Cell.* **93**:177–188.
13. Lu, W., et al. 1997. Perinatal lethality with kidney and pancreas defects in mice with a targetted Pkd1 mutation. *Nat. Genet.* **17**:179–181.
14. Muto, S., et al. 2002. Pioglitazone improves the phenotype and molecular defects of a targeted Pkd1 mutant. *Hum Mol Genet* **11**:1731–1742.
15. Boulter, C., et al. 2001. Cardiovascular, skeletal, and renal defects in mice with a targeted disruption of the Pkd1 gene. *Proc. Natl. Acad. Sci. U. S. A.* **98**:12174–12179.
16. Lu, W., et al. 2001. Comparison of Pkd1-targeted mutants reveals that loss of polycystin-1 causes cystogenesis and bone defects. *Hum. Mol. Genet.* **10**:2385–2396.
17. Sutters, M., and Germino, G.G. 2003. Autosomal dominant polycystic kidney disease: molecular genetics and pathophysiology. *J. Lab. Clin. Med.* **141**:91–101.
18. Igarashi, P., and Somlo, S. 2002. Genetics and pathogenesis of polycystic kidney disease. *J. Am. Soc. Nephrol.* **13**:2384–2398.
19. Nauli, S.M., et al. 2003. Polycystins 1 and 2 mediate mechanosensation in the primary cilium of kidney cells. *Nat. Genet.* **33**:129–137.
20. Yoder, B.K., Hou, X., and Guay-Woodford, L.M. 2002. The polycystic kidney disease proteins, polycystin-1, polycystin-2, polaris, and cystin, are co-localized in renal cilia. *J. Am. Soc. Nephrol.* **13**:2508–2516.
21. Lin, F., et al. 2003. Kidney-specific inactivation of the KIF3A subunit of kinesin-II inhibits renal ciliogenesis and produces polycystic kidney disease. *Proc. Natl. Acad. Sci. U. S. A.* **100**:5286–5291.
22. McGrath, J., Somlo, S., Makova, S., Tian, X., and Brueckner, M. 2003. Two populations of node monocilia initiate left-right asymmetry in the mouse. *Cell.* **114**:61–73.
23. Lubarsky, B., and Krasnow, M.A. 2003. Tube morphogenesis: making and shaping biological tubes. *Cell.* **112**:19–28.
24. Grantham, J.J., Geiser, J.L., and Evan, A.P. 1987. Cyst formation and growth in autosomal dominant polycystic kidney disease. *Kidney Int.* **31**:1145–1152.
25. Nadasdy, T., et al. 1995. Proliferative activity of cyst epithelium in human renal cystic diseases. *J. Am. Soc. Nephrol.* **5**:1462–1468.
26. Lanoix, J., D'Agati, V., Szabolcs, M., and Trudel, M. 1996. Dysregulation of cellular proliferation and apoptosis mediates human autosomal dominant polycystic kidney disease (ADPKD). *Oncogene.* **13**:1153–1160.
27. Wilson, P.D., Du, J., and Norman, J.T. 1993. Autocrine, endocrine and paracrine regulation of growth abnormalities in autosomal dominant polycystic kidney disease. *Eur. J. Cell Biol.* **61**:131–138.
28. Yamaguchi, T., et al. 2003. Cyclic AMP activates B-Raf and ERK in cyst epithelial cells from autosomal-dominant polycystic kidneys. *Kidney Int.* **63**:1983–1994.
29. Hanaoka, K., and Guggino, W.B. 2000. cAMP regulates cell proliferation and cyst formation in autosomal polycystic kidney disease cells. *J. Am. Soc. Nephrol.* **11**:1179–1187.
30. Bhunia, A.K., et al. 2002. PKD1 induces p21(waf1) and regulation of the cell cycle via direct activation of the JAK-STAT signaling pathway in a process requiring PKD2. *Cell.* **109**:157–168.
31. Ong, A.C., et al. 1999. Polycystin-1 expression in PKD1, early-onset PKD1, and TSC2/PKD1 cystic tissue. *Kidney Int.* **56**:1324–1333.
32. Ward, C.J., et al. 1996. Polycystin, the polycystic kidney disease 1 protein, is expressed by epithelial cells in fetal, adult, and polycystic kidney. *Proc. Natl. Acad. Sci. U. S. A.* **93**:1524–1528.
33. Geng, L., et al. 1996. Identification and localization of polycystin, the PKD1 gene product. *J. Clin. Invest.* **98**:2674–2682.
34. Griffin, M.D., Torres, V.E., Grande, J.P., and Kumar, R. 1996. Immunolocalization of polycystin in human tissues and cultured cells. *Proc Assoc Am Physicians.* **108**:185–197.
35. Weston, B.S., et al. 1997. Polycystin expression during embryonic development of human kidney in adult tissues and ADPKD tissue. *Histochem J* **29**:847–856.
36. Nauta, J., Goedbloed, M.A., van den Ouweland, A.M., Nellist, M., and Hoogeveen, A.T. 2000. Immunological detection of polycystin-1 in human kidney. *Histochem. Cell Biol.* **113**:303–311.
37. Zambrowicz, B.P., et al. 1997. Disruption of overlapping transcripts in the ROSA beta geo 26 gene trap strain leads to widespread expression of beta-galactosidase in mouse embryos and hematopoietic cells. *Proc. Natl. Acad. Sci. U. S. A.* **94**:3789–3794.
38. Todaro, G.J., and Green, H. 1963. Quantitative studies of the growth of mouse embryo cells in culture and their development into established lines. *J. Cell Biol.* **17**:299–313.
39. Kamijo, T., et al. 1997. Tumor suppression at the mouse INK4a locus mediated by the alternative reading frame product p19ARF. *Cell.* **91**:649–659.
40. Loghman-Adham, M., Nauli, S.M., Soto, C.E., Kariuki, B., and Zhou, J. 2003. Immortalized epithelial cells from human autosomal dominant polycystic kidney cysts. *Am. J. Physiol. Renal Physiol.* **285**:F397–F412.
41. Bernstein, J., and Gilbert-Barness, E. 1994. Congenital malformation of the kidney. In *Renal pathology.* B. Brenner, editor. J.B. Lippincott Co. Philadelphia, Pennsylvania, USA. 1366 pp.
42. Huan, Y., and van Adelsberg, J. 1999. Polycystin-1, the PKD1 gene product, is in a complex containing E-cadherin and the catenins. *J. Clin. Invest.* **104**:1459–1468.
43. Kim, H., Bae, Y., Jeong, W., Ahn, C., and Kang, S. 2004. Depletion of PKD1 by an antisense oligodeoxynucleotide induces premature G1/S-phase transition. *Eur. J. Hum. Genet.* **12**:433–440.
44. Gartel, A.L., and Tyner, A.L. 1999. Transcriptional regulation of the p21((WAF1/CIP1)) gene. *Exp. Cell Res.* **246**:280–289.
45. Thomson, R.B., et al. 2003. Histopathological analysis of renal cystic epithelia in the Pkd2WS25/- mouse model of ADPKD. *Am. J. Physiol. Renal Physiol.* **285**:F870–F880.
46. Woo, D. 1995. Apoptosis and loss of renal tissue in polycystic kidney diseases. *N. Engl. J. Med.* **333**:18–25.
47. Arnould, T., et al. 1998. The polycystic kidney disease 1 gene product mediates protein kinase C alpha-dependent and c-Jun N-terminal kinase-dependent activation of the transcription factor AP-1. *J. Biol. Chem.* **273**:6013–6018.
48. Wood, S.A., Allen, N.D., Rossant, J., Auerbach, A., and Nagy, A. 1993. Non-injection methods for the production of embryonic stem cell-embryo chimaeras. *Nature.* **365**:87–89.
49. Kojima, S., et al. 2001. Testicular germ cell apoptosis in Bcl6-deficient mice. *Development* **128**:57–65.

Reprinted from ANNALS OF RHEUMATIC DISEASES, August 2005, Vol 64, p 1165-1173

EXTENDED REPORT

# Up regulated expression of tumour necrosis factor α converting enzyme in peripheral monocytes of patients with early systemic sclerosis

**T Bohgaki, Y Amasaki, N Nishimura, M Bohgaki, Y Yamashita, M Nishio, K-i Sawada, S Jodo, T Atsumi, T Koike**

*Ann Rheum Dis* 2005;**64**:1165–1173. doi: 10.1136/ard.2004.030338

See end of article for authors' affiliations

Correspondence to: Dr Y Amasaki, Department of Medicine II, Hokkaido University Graduate School of Medicine, Address: N-15 W-7, Kita-ku, Sapporo 060-8638, Japan; yamasaki@med.hokudai.ac.jp

Accepted 28 December 2004

**Background:** Systemic sclerosis (SSc) is accompanied by abnormalities in humoral and cellular immune systems.
**Objective:** To determine the genes specifically expressed in the immune system in SSc by analysis of the gene expression profile of peripheral blood mononuclear cells (PBMC) from patients with SSc, including those treated with haematopoietic stem cell transplantation (HSCT). Additionally, to investigate the clinical significance of the up regulation of tumour necrosis factor α (TNFα) converting enzyme (TACE).
**Methods:** PBMC from patients with SSc (n = 23) and other autoimmune diseases (systemic lupus erythematosus (SLE, n = 16), rheumatoid arthritis (RA, n = 29)), and from disease-free controls (n = 36) were examined. Complementary DNA arrays were used to evaluate gene expression of PBMC, in combination with real time quantitative polymerase chain reactions. TACE protein expression in PBMC was examined by fluorescence activated cell sorter (FACS).
**Results:** In patients with SSc 118 genes were down regulated after HSCT. Subsequent comparative analysis of SSc without HSCT and healthy controls indicated SSc-specific up regulation for three genes: monocyte chemoattractant protein-3 ($p = 0.0015$), macrophage inflammatory protein 3α ($p = 0.0339$), and TACE ($p = 0.0251$). In the FACS analysis, TACE protein was mainly expressed on $CD14^+$ monocytes both in patients with SSc and controls. TACE expression on $CD14^+$ cells was significantly increased in patients with early SSc ($p = 0.0096$), but not in those with chronic SSc, SLE, or RA. TACE protein levels in SSc monocytes correlated with the intracellular CD68 levels ($p = 0.0016$).
**Conclusions:** Up regulation of TACE expression was a unique profile in early SSc, and may affect the function of TNFα and other immunoregulatory molecules.

Systemic sclerosis (SSc) is a multisystem disorder of connective tissue. Increased biosynthesis of multiple matrix proteins by interstitial fibroblasts is the hallmark of SSc, with development of skin sclerosis and involvement of visceral organs.[1] The pathogenesis of SSc includes vasculopathy associated with endothelial cell dysfunction, and extensive fibrosis secondary to fibroblast activation.[2 3] Functional abnormality in T and B lymphocytes has been considered in the pathogenesis, based on the presence of disease-specific autoantibodies and hypergammaglobulinaemia in SSc.[4 5] Growth factors and cytokines are also thought to play a part in the progression of connective tissue fibrosis in SSc. Among them, transforming growth factor β (TGFβ) and the Smad system have a central role in the SSc dermis.[6] However, the molecular basis of the pathogenesis of SSc has remained unclear.

The use of gene expression profiling, such as the complementary DNA (cDNA) array system, is increasingly being used for various diseases, and is used in the aetiological study of SSc.[7 8] Increased expression of several genes has been suggested, but a disease-specific gene profile of SSc has not yet been determined, possibly owing to the difficulty of achieving disease remission in SSc, which is necessary for a comparative analysis of the active and disease-free status. Recently, the efficacy of high dose chemotherapy after autologous haematopoietic stem cell transplantation (HSCT) for refractory autoimmune diseases has been reported.[9 10] HSCT has been performed in a number of cases of SSc, with good results.[11–13] When we performed autologous CD34 selected HSCT for our patients with SSc, we observed a prompt and persistent improvement of skin sclerosis and stabilisation of organ disease. Under this condition, it was possible to carry out a comparative analysis of gene expression profile between an active (pre-HSCT) and a remission status (post-HSCT) in the same patient with SSc.

We studied the gene expression profile in peripheral blood mononuclear cells (PBMC) from patients with SSc treated with HSCT, and found that expression of tumour necrosis factor α (TNFα) converting enzyme (TACE) was increased in circulating monocytes from patients with SSc. The correlation

**Abbreviations:** Ab, antibody; aCENP-B Ab, anticentromere protein-B Ab; ACR, American College of Rheumatology; ANA, antinuclear Ab; aRNP Ab, anti-ribonucleoprotein Ab; aTopo-I Ab, antitopoisomerase I Ab; CaMKIIβ, calcium/calmodulin dependent protein kinase II β; cDNA, complementary DNA; CRP, C reactive protein; CTGF, connective tissue growth factor; FACS, fluorescence activated cell sorter; FITC, fluorescein isothiocyanate; FSC, forward light scatter; GAPDH, glyceraldehyde-3-phosphate dehydrogenase; HSCT, haematopoietic stem cell transplantation; IL, interleukin; MCP, monocyte chemoattractant protein; MFI, mean fluorescence intensity; mIgG1, isotype matched control mouse IgG1; MIP, macrophage inflammatory protein; mRNA, messenger RNA; NF-κB, nuclear factor-κB; NIK, NF-κB inducing kinase; PBMC, peripheral blood mononuclear cells; PE, phycoerythrin; RA, rheumatoid arthritis; real time PCR, quantitative TaqMan real time polymerase chain reaction; RGS, regulators of G-protein signalling; SLE, systemic lupus erythematosus; SSc, systemic sclerosis; SSC, side light scatter; TACE, tumour necrosis factor α converting enzyme; TGFβ, transforming growth factor β; TNFα, tumour necrosis factor α; TNF-R, TNF receptor

**Table 1** Clinical features of the study subjects*

| Characteristics | SSc (n = 20) | SSc treated with HSCT (n = 3) | RA (n = 29) | SLE (n = 16) | Controls (n = 36) |
|---|---|---|---|---|---|
| Sex (female/male) | 17/3 | 2/1 | 23/6 | 14/2 | 25/11 |
| Age (years), mean (SD) | 51.0 (12.6) | 43.3 (21.1) | 58.9 (14.4) | 40.5 (13.4) | 40.0 (11.5) |
| Duration of disease (months), median (min–max) | 41.0 (6–278) | 18 (12–24) | 36.0 (3–360) | 144.0 (1–444) | |
| Prednisolone (mg/day), mean (min–max) | 0.875 (0–10) | 0.83 (0–2.5) | 4.1 (0–25) | 13.0 (0–60) | |
| Organ involvement, No (%) | | | | | |
| Lung | 13 (65) | 2 (67) | 3 (10) | 0 (0) | |
| Muscle | 1 (5) | 0 (0) | 0 (0) | 0 (0) | |
| Joint | 8 (40) | 0 (0) | 29 (100) | 3 (19) | |
| Renal | 1 (5) | 1 (33) | 0 (0) | 5 (31) | |
| Cardiac | 2 (10) | 0 (0) | 0 (0) | 0 (0) | |
| Serology, No (%) | | | | | |
| ANA | 19 (95) | 2 (67) | 19 (66) | 16 (100) | |
| aTopo-I Ab | 11 (55) | 2 (67) | N/A | N/A | |
| aCENP-B Ab | 2 (10) | 0 (0) | N/A | N/A | |
| aRNP Ab | 1 (5) | 0 (0) | N/A | 11 (69) | |

*The SSc groups consisted of 20 subjects, and three patients treated with HSCT. In these three patients with HSCT, RNA samples were obtained before (<1 month before mobilisation) and after HSCT.
Organ involvements in this study were defined as: lung (interstitial pneumonia proved by high resolution computed tomography), muscle (increased serum creatinine kinase or serum aldolase, or both, continuously), joint (arthralgia or arthritis, or both), renal (renal crisis in patients with SSc and nephritis in RA and SLE), cardiac (arrhythmia).[18–22]
N/A, not available.

of TACE expression with the clinical findings in patients with SSc was analysed and is discussed below.

## PATIENTS AND METHODS

### Patients and controls

Twenty three Japanese patients with SSc who fulfilled the 1980 criteria of the American College of Rheumatology (ACR) were assessed in this study.[14] These patients were categorised as those with diffuse cutaneous type disease characterised by generalised or widespread skin thickening.[15] Table 1 summarises their clinical features. Patients were classified as having early SSc (n = 12) if the disease duration after the appearance of the first non-Raynaud's phenomenon was within 3 years.[11] Other patients with SSc with a longer disease duration were classified as having chronic SSc (n = 11). Of the 12 patients with early SSc, three were treated with HSCT using autologous $CD34^+$ selected peripheral blood stem cells; blood samples were obtained throughout the clinical course. Other patients with autoimmune diseases had rheumatoid arthritis (RA) or systemic lupus erythematosus (SLE). These patients fulfilled the criteria of the ACR, respectively.[16 17] As healthy controls, 36 disease-free Japanese volunteers, mean (SD) age 40.0 (11.5) years, were enrolled in the study.

### Study design

To search for specific genes which changed between the active and remission status, before and after HSCT, we first analysed gene expression profiles of PBMC from patients treated with HSCT using cDNA array (n = 3). Next, specific up regulated genes in patients with SSc were explored using cDNA array by comparing mRNA levels in PBMC of patients with SSc who had not received HSCT (n = 6) and healthy controls (n = 5). Specific gene candidates were confirmed by real time polymerase chain reaction (PCR) in patients with SSc without HSCT (n = 9) and controls (n = 6). Finally, protein expression levels were analysed by a fluorescence activated cell sorter (FACS) analysis.

### PBMC isolation

Blood sampling was carried out after obtaining written informed consent according to the guidelines of the ethical committee of Hokkaido University. PBMC were obtained from heparinised venous blood, using gradient centrifugation over Ficoll-Paque Plus (Amersham Biosciences Corp, NJ).

### RNA extraction and cDNA array analysis

Total RNAs from PBMC were isolated using TRIzol reagent (Invitrogen, Carlsbad, CA). Poly(A) RNA was isolated from total RNA using a MagExtractor (TOYOBO, Osaka, Japan), and poly(A) RNA (2 μg) was reverse transcribed by ReverTraAce (TOYOBO), in the presence of cDNA synthesis primers and biotin-16-deoxyuridine triphosphate (TOYOBO), according to the manufacturer's instructions. cDNA array analysis was performed using human cDNA expression filters (Human Immunology Filters (TOYOBO)), on which 621 species of human cDNA fragments and housekeeping genes are spotted in duplicate: (http://www.toyobo.co.jp/seihin/xr/product/genenavi/genenavigator.html, accessed 5 May 2005)). Hybridisation and subsequent cDNA array analyses were carried out as described previously,[23] with some modification. Briefly, after standard prehybridisation, cDNA array filters were hybridised with a biotin labelled cDNA probe in PerfectHyb solution (TOYOBO) overnight at 68°C. After washing under conditions of high stringency, specific signals on the filters were visualised using Phototope-Star Detection Kits (New England Biolabs, Beverly, MA). Fluorescence signals for mRNA expression levels were obtained using a Fluor-S Multiimager system (Nippon Bio-Rad Laboratories, Tokyo, Japan). The signal intensity among filters was compared in an E-Gene Navigator Analysis (GeneticLab, Sapporo, Japan), and was expressed as an mRNA expression index to the intensity of the internal glyceraldehyde-3-phosphate dehydrogenase (GAPDH) gene expression.

### Quantitative TaqMan real time polymerase chain reaction (real time PCR)

A two step PCR was carried out on serial dilutions of cDNA samples from PBMC from the patients with SSc and the controls. Real time PCR amplification and determination of cDNA transcripts were carried out with the ABI PRISM 7000 sequence detection system (Applied Biosystems, Foster City, CA) and gene-specific sets of TaqMan Universal PCR master mix and assays-on-demand gene expression probes (Applied Biosystems).

**Table 2** Down regulated genes expressed in PBMC from patients with SSc at 6 months after HSCT as indicated by a cDNA array

| Gene name | Accession No | Gene name | Accession No | Gene name | Accession No |
|---|---|---|---|---|---|
| Bik | X89986 | MCP-2 | Y16645 | GRP94 | X15187 |
| Caspase-8 | U60520 | MCP-3 | X72308 | HSP105β | AB003333 |
| JunB | X51345 | Neurophysin II | X03172 | MMP3 | J03209 |
| AP-β | X95694 | Delta | AF003522 | TACE | U86755 |
| AP-γ | X95693 | Angiotensinogen | K02215 | Cathepsin G | M16117 |
| Erg-1 | M21535 | Gonadotropin α peptide | V00518 | Pin1 | U49070 |
| GLI-3 | M57609 | Somatostatin | J00306 | Calpastatin | U26724 |
| IκBα | M69043 | VIP | M36634 | Moesin | M69066 |
| IRF-2 | X15949 | Gastrin | V00511 | Radixin | L02320 |
| N-Myc | M13228 | IP10 | X02530 | LAT | AF036905 |
| Per2 | AB002345 | MIP-3α | U77035 | Fyb | AF001862 |
| Pax5 | M96944 | EphA5 | L36644 | Furin | X17094 |
| LXRα | U22662 | EphB6 | D83492 | PAI-2 | M16006 |
| RXRγ | U38480 | Insulin receptor | M10051 | CD3γ | X04145 |
| RAC3 | AF010227 | MC1-R | X67594 | CD3ε | X03884 |
| PPARγ | L40904 | MC4-R | L08603 | CD3ζ | J04132 |
| MCR | M16801 | β2-AR | M15169 | CD8β 1 | X13444 |
| MEK-5 | U25265 | FRP-3 | U24163 | CD5 | X04391 |
| MEK kinase-2 | AF111105 | Notch 2 | AF097645 | CD72 | M54992 |
| Raf-1 | X03484 | Thrombin R | M62424 | CD6 | X60992 |
| Raf-B | M95712 | IFNγR2 | U05875 | CD7 | X06180 |
| KKIAMRE | U35146 | IL2Rγ | D11086 | CD20 | X12530 |
| Rhotekin | AI970663 | IL15Rα | U31628 | CD27 | M63928 |
| IKKα | AF080157 | c-Kit | X06182 | CD28 | J02988 |
| JAK1 | M64174 | CXCR-4 | AF025375 | CD35 | Y00816 |
| MuSK | AF006464 | Slap | D89077 | CD38 | M34461 |
| TGFβ2 | M19154 | Shb | X75342 | CD40L | L07414 |
| GDF-8 | AF019627 | Sos1 | L13858 | CD42a | X52997 |
| Inhibin α | M13981 | Dbl | J03639 | CD43 | J04168 |
| FGF-1 | X51943 | Ral GDS | U14417 | CD46 BC1 | M58050 |
| FGF-5 | M37825 | RGS4 | U27768 | CD59 | X16447 |
| FGF-6 | X63454 | PI4-Kα | AJ011121 | CD69 | L07555 |
| HGF β chain | E08541 | FRP1 | U49844 | CD74 | X03339 |
| IGF-BP3 | M35878 | Sam68 | M88108 | TCRα | U36759 |
| TNFβ | D12614 | PPP1CA | X70848 | TCRβ | L07294 |
| IL2 | U25676 | CD45 | Y00062 | TCRγ | Y00790 |
| IL10 | M57627 | p120 | AF062343 | CD138 | J05392 |
| IL15 | AF031167 | Ref-1 | D90373 | ICAM3 | X69819 |
| IL18 | D49950 | HSP60 | M34664 | | |
| SCF | M59964 | HSP90β | M16660 | | |

One hundred and eighteen gene expressions decreased more than 20% in all three patients with SSc treated with HSCT at 6 months after HSCT compared with before HSCT (<1 month before mobilisation) by cDNA array analysis. Changes in white blood cell and monocyte counts in PBMC from three patients with SSc treated with HSCT were from 4867 (116)/μl to 5100 (917)/μl (p=0.5105*) and from 506 (157)/μl to 589 (44) /μl (p=0.7106*), respectively. *Paired *t* test.

### FACS analysis

The following mouse monoclonal antibodies were purchased from BD Biosciences Pharmingen (San Diego, CA): anti-human CD3-Cy-chrome, CD4-fluorescein isothiocyanate (FITC), CD8-phycoerythrin (PE) and FITC, CD56-FITC, CD19-FITC, CD68-PE, and CD69-PE. Monoclonal mouse antihuman-CD14-FITC, CD71-PE (Beckman Coulter Inc, Fullerton, CA) and antihuman TACE-PE (R&D systems, Abingdon, UK) were also used for surface immunostaining of the cells. The specificity of antihuman TACE has been characterised.[24] In the case of CD68, intracellular staining was done using Cytofix/Cytoperm Plus (BD Biosciences Pharmingen, San Diego, CA), according to the manufacturer's instructions. After washing twice with phosphate buffered saline (PBS), cells were subjected to FACS analysis of immunostained cells using a FACSCalibur flow cytometer (Becton Dickinson Immunocytometry Systems, San Jose, CA).

### Statistical analysis and clinical significance

Calculations were made using the statistical software package StatView 5.0 (Abacus Concepts, Berkeley, CA). Comparisons of mRNA expression of PBMC were made using Mann-Whitney statistics. Group mean comparisons of the TACE protein expression levels, represented by mean fluorescence intensity (MFI), and TACE positive cells were based on Kruskal-Wallis H statistics. A paired *t* test was used to analyse the difference in blood cell counts of patients with SSc before and after HSCT. The data are presented as the means (SD). Differences were examined based on analysis of variance, and p values $<0.05$ were considered significant.

## RESULTS

### Comprehensive analysis of up regulated genes in PBMC from patients with SSc using cDNA array and real time PCR

We first analysed mRNA expression in PBMC from three patients with SSc treated with HSCT, in order to search for genes with expression levels down regulated after this treatment. In these patients, skin involvement, as expressed by the modified Rodnan total thickness skin score improved significantly by 54% (from 30.3 (6.8) to 12.6 (13.2)) and the modified Health Assessment Questionnaire improved by 22.8% (from 1.67 (0.88) to 1.29 (1.04)) at 6 months after effective HSCT. This improvement persisted even 3 years after this treatment. PBMC specimens were obtained from these patients before (<1 month before mobilisation) and 6 months after HSCT, and were processed for mRNA extraction followed by cDNA array analyses.

**Table 3** Up regulated genes expressed in PBMC from patients with SSc without HSCT as indicated by a cDNA array

| Classification | Up regulated genes | GenBank accession No | Ratio (fold increase) |
|---|---|---|---|
| Regulatory transcription factors | Per1 | AB002107 | 7.61 |
| | Erg-3 | S40832 | 4.50 |
| | Gfi-1 | U67369 | 4.44 |
| Protein kinases | CaMKIIβ | AF078803 | 4.90 |
| Growth factors and hormones | IL1β* | X02532 | 9.70 |
| | MIP-1β* | J04130 | 6.58 |
| | TARC | D43767 | 5.56 |
| | IL12p35 | AF180562 | 4.27 |
| | MIP-3α* | U77035 | 4.25 |
| | MCP-3* | X72308 | 3.88 |
| Membrane receptors | IL15Rα | U31628 | 3.46 |
| Signalling intermediates | Gab1 | U43885 | 6.09 |
| | RGS-1* | X73427 | 5.21 |
| | Shb | X75342 | 4.32 |
| | TACE* | U86755 | 3.70 |
| | Dbl | J03639 | 3.38 |
| Lymphocyte signalling | CD34 | M81104 | 3.40 |

The ratio of the gene expression index (see "Patients and methods") of patients with SSc without HSCT (n = 6) to healthy controls (n = 5) was calculated, and the list of up regulated genes using cDNA array (with an SSc/control ratio >3.0) is displayed. *Gene expression was confirmed by real time PCR.
CaMKIIβ, calcium/calmodulin dependent protein kinase II β; MIP-1β, macrophage inflammatory protein β; MCP-3, monocyte chemoattractant protein-3; RGS-1, regulators of G-protein signalling-1.

At 6 months after this treatment, down regulation of mRNA expression levels was seen in 118 genes using cDNA array (table 2). In patients with SSc without HSCT, 17 genes were specifically up regulated compared with controls (table 3). In addition, the profile of mRNA expression between baseline and after 6 months in patients with SSc without HSCT was very similar, thus a "natural state for 6 months" did not modify the mRNA levels examined in this study (data not shown). Real time PCR showed that only four gene expression levels had statistical significance as disease-specific genes in 17 patients with SSc who had not received HSCT (fig 1). As a result, gene expression levels of monocyte chemoattractant protein (MCP)-3, macrophage inflammatory protein (MIP)-3α, and TACE were down regulated after HSCT in the cDNA array and up regulated specifically in patients with SSc without HSCT by real time PCR (fig 2). In this study, we further investigated the expression of TACE, which has a crucial role in the immune system. A role for chemokines, including MCP and MIP families, in the pathogenesis of scleroderma has been suggested (reviewed by Atamas and White[25]).

## Cell surface TACE expression

We first examined PBMC from healthy controls for the expression of TACE protein. In PBMC from healthy subjects, a small population was brightly stained by an antihuman TACE monoclonal antibody (fig 3A). Multicolour FACS analyses showed that surface TACE expression was barely detectable on $CD4^+CD3^+$, $CD8^+CD3^+$, $CD19^+$, and $CD56^+$ populations. In contrast, surface TACE expression was detected on the $CD14^+$ population (fig 3B). It was confirmed that these $CD14^+$ populations were monocytes, by profiles of forward and side light scatter (SSC), as well as by intracellular CD68 protein expression. Surface TACE expression levels on monocytes were not affected by the age and sex of the controls (data not shown).

We next investigated expression levels of TACE protein in subsets of PBMC from patients with SSc. In these patients, surface TACE expression was also detected on monocytes but not on $CD4^+CD3^+$, $CD8^+CD3^+$, $CD19^+$, and $CD56^+$ populations, respectively (data not shown). Figure 3C shows representative FACS profiles of TACE protein expression for $CD14^+$

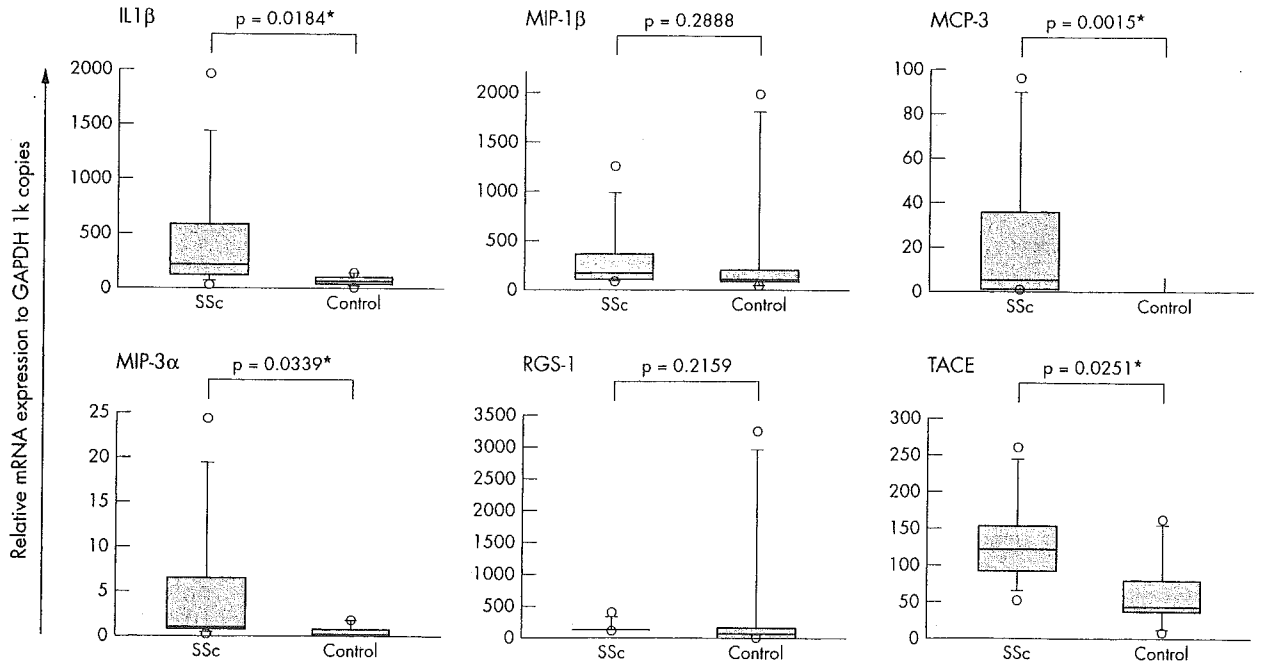


**Figure 1** Quantitative analysis of up regulated genes in PBMC from patients with SSc, assessed using real time PCR. cDNA specimen from patients with SSc (n = 9) and disease-free volunteers (n = 6) were analysed for six genes species (TACE, interleukin (IL) 1β, MIP-3α, MIP-1β, MCP-3, and a regulator of G-protein signalling (RGS)-1), indicated from the cDNA array study (table 3). *$p<0.05$.

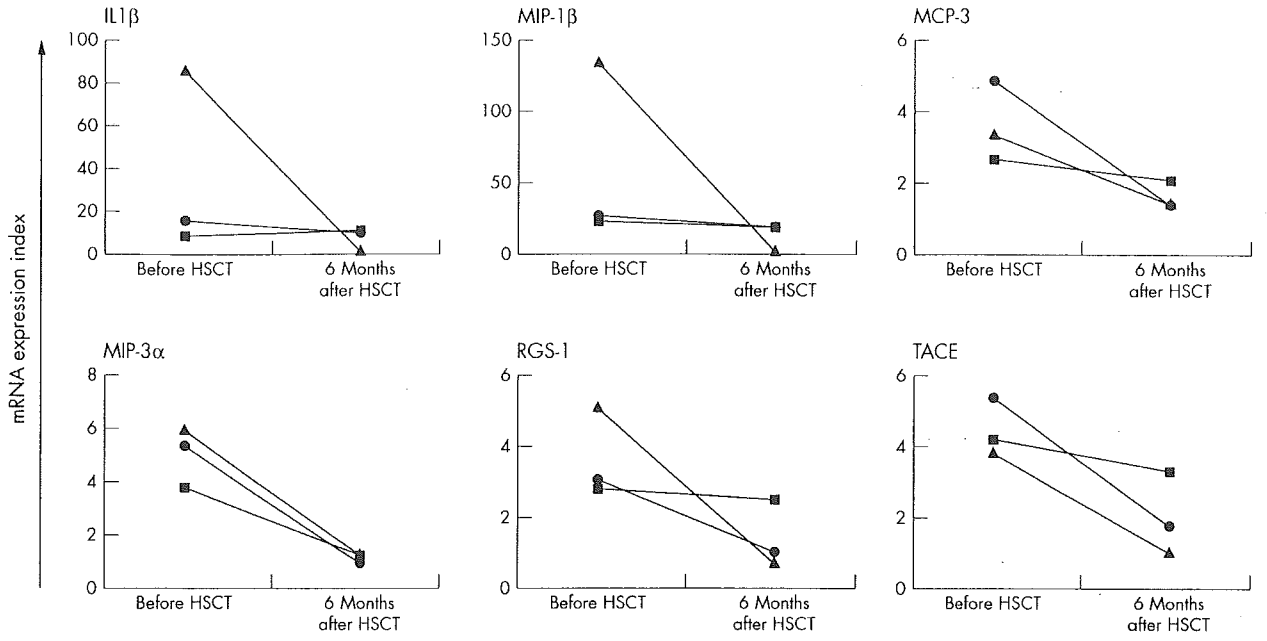


**Figure 2** Changes of mRNA expression levels of IL1β, MIP-1β, MCP-3, MIP3-α, RGS-1, and TACE in patients with SSc before and after HSCT using cDNA array. RNA specimens were obtained from individual patients before (<1 month before mobilisation) and 6 months after HSCT. Relative expression levels of mRNA were determined using cDNA arrays performed simultaneously. The expression levels of each cDNA transcript were displayed as a relative mRNA expression index compared with the levels of internal GAPDH gene expression, as described in "Patients and methods".

monocytes. In the patients with SSc, TACE expression in monocytes was significantly increased in comparison with findings in healthy controls, and in patients with RA and SLE (fig 3C). When analysed statistically, cell surface TACE protein levels of monocytes and TACE positive cells in peripheral blood were significantly increased in patients with SSc, especially in patients with early SSc with disease duration of <3 years, in comparison with controls and patients with non-SSc autoimmune diseases, as well as those with chronic SSc (fig 4). In addition, TACE protein levels correlated with mRNA expression levels by real time PCR ($r = 0.640$, $p = 0.0462$). Thus, we concluded that up regulated expression of TACE protein by monocytes was a unique profile of early SSc.

### Relationship between cell surface TACE expression and maturation/activation markers of monocytes

To better understand the mechanism of TACE up regulation in monocytes in SSc, we next investigated correlations between TACE and activation/differentiation markers of monocytes from patients with SSc. Coexpression of surface CD69, CD71, and intracellular CD68 with TACE was evaluated using FACS analysis (fig 5). These proteins were variously expressed on SSc monocytes, but only intracellular CD68 protein levels showed a significant correlation with cell surface TACE protein expression levels ($r = 0.671$, $p = 0.0016$), while cell surface CD69 and CD71 proteins did not correlate.

### Association of cell surface TACE expression levels with clinical features of SSc

We then analysed the correlation of cell surface TACE protein levels of monocytes from patients with SSc (including patients with early and chronic disease) with clinical features of the disease. The expression levels of TACE protein on monocytes in patients with SSc, however, did not significantly correlate with titres of autoantibodies, including antinuclear Ab (ANA), antitopoisomerase I Ab (aTopo-I Ab), anticentromere protein-B Ab (aCENP-B Ab), anti-ribonucleoprotein Ab (aRNP Ab), as well as levels of serum immunoglobulins. The TACE protein levels did not correlate either with CRP in patients with SSc (fig 4, $r = -0.216$, $p = 0.3599$). The expression levels of TACE protein did not differ significantly between patients with SSc with or without visceral organ disease, including interstitial pneumonia and gastrointestinal complications (data not shown).

## DISCUSSION

HSCT can be an effective treatment for subjects with severe autoimmune diseases, including SSc.[11–13] In our three patients with SSc who received HSCT, significant improvement of skin sclerosis was promptly achieved and persisted without any immunosuppressant drug treatment. In such patients, the gene expression profile can be studied comparatively between the active and remission state of SSc, with a minimum background of therapeutic reagents. In this study we performed a cDNA analysis of PBMC from patients with SSc who had undergone HSCT. After extensive analyses, up regulation of MCP-3, MIP-3α, and TACE in PBMC from patients with SSc who had not had HSCT was evident.

It was notable that these genes are commonly expressed by monocytes/macrophages. In SSc, although the earliest pathological events include dysfunction of microvascular systems and dermal fibroblasts,[26 27] cells and factors that mediate such abnormalities have not been defined. Histological studies of early SSc showed that cells infiltrating the skin of patients with early stage SSc are mainly $CD14^+$ monocytes/macrophages,[28 29] indicating the crucial role of these cells.

A role for chemokines has been suggested in the pathogenesis of SSc.[25 30–32] Our observation about MCP-3 and MIP-3α in PBMC from patients with SSc in this study is consistent with previous findings.[33–35]

In addition, overexpression of TACE in PBMC appeared to be a new hallmark of early stage SSc. In PBMC subpopulations, TACE protein expression was almost limited to

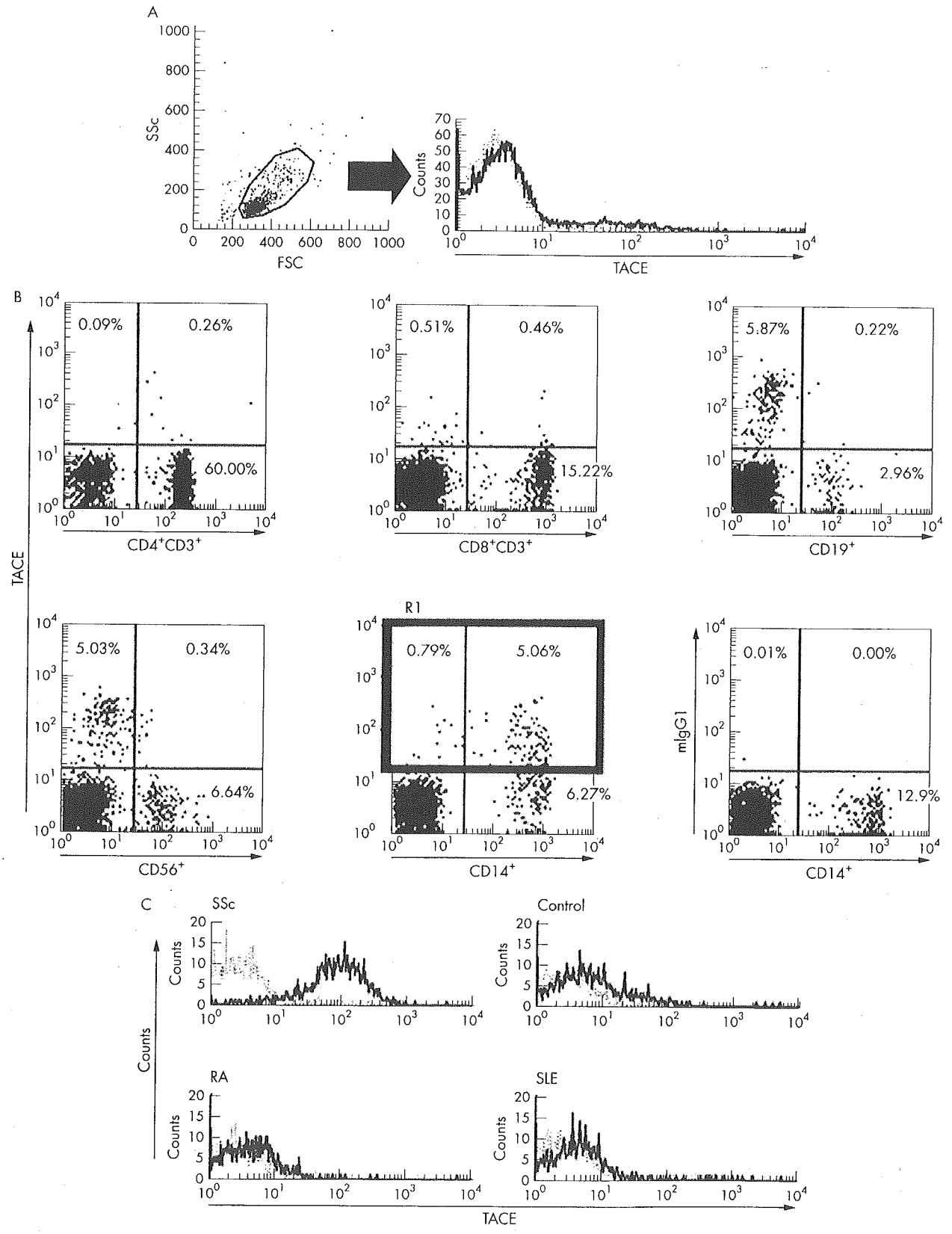


**Figure 3** Expression of TACE protein in PBMC of healthy controls and patients. (A, left panel) A small population was detected in a high fluorescence intensity. (A, right panel) Solid line, cells stained with anti-TACE monoclonal Ab; dotted line, cells stained with isotype matched control mouse IgG1 Ab. (B) Expression of TACE protein in PBMC subsets from a healthy control. (C) Representative cell surface expression of TACE protein on monocytes from patients with autoimmune diseases and controls. Solid line, cells stained with anti-TACE monoclonal Ab; dotted line, cells stained with mIgG1 Ab. Results are representative of three independent experiments.

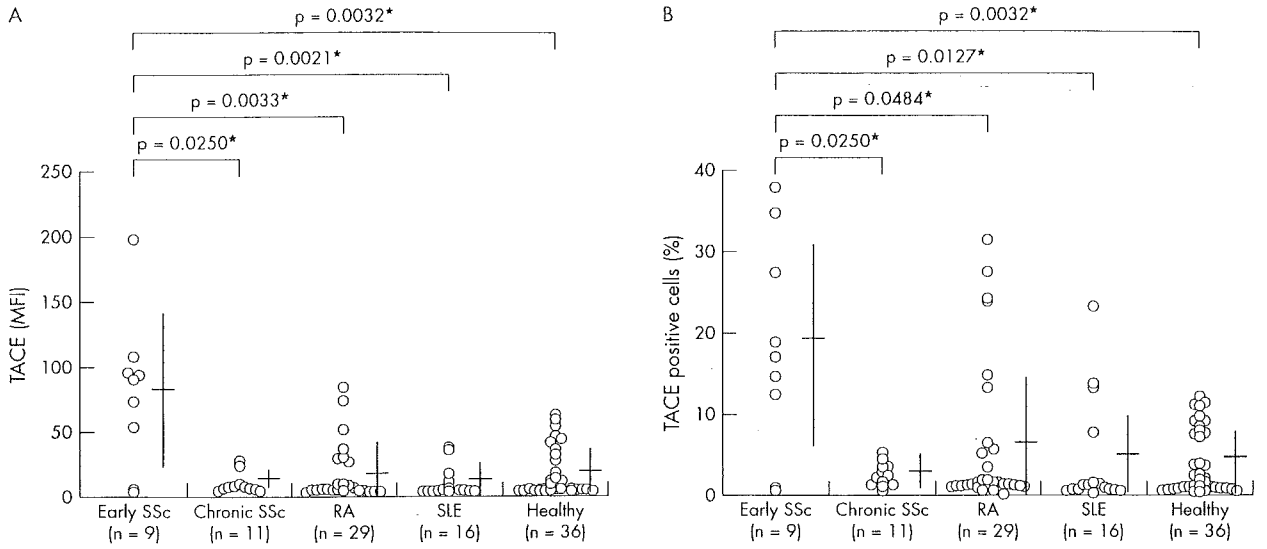


**Figure 4** (A) Comparison of cell surface TACE expression by monocytes of patients with early SSc, chronic SSc, RA, SLE, and healthy controls. Cell surface expression levels of TACE were evaluated using FACS, gating on monocytes by forward and side light scatter and on $CD14^+$ cells. The levels of TACE protein expression were represented by the MFI. mIgG1 Ab-PE staining was performed in all measurements, and showed identical levels of background staining. *$p<0.05$, ($p=0.0065$ (Kruskal-Wallis H statistics)). (B) Comparison of TACE positive cells in PBMC of patients with early SSc, chronic SSc, RA, SLE, and healthy controls evaluated using FACS. TACE positive cells were defined on gate R1 in fig 3B. *$p<0.05$.

monocytes (fig 3B), whereas widespread distribution of TACE mRNA in tissue was suggested and its expression of protein levels in blood cells has not been yet described in detail.[36 37] TACE protein levels on monocytes were significantly higher in SSc than in controls (figs 3C and 4), suggesting a possible association between TACE and the function of TACE-expressing monocytes with the pathoaetiology of SSc. In autoimmune diseases, up regulation of TACE in inflammatory synovial tissue from patients with RA and increased TACE mRNA expression in PBMC of patients with multiple sclerosis have been suggested, but the disease specificity has been unclear.[38–40] Our report provides the first

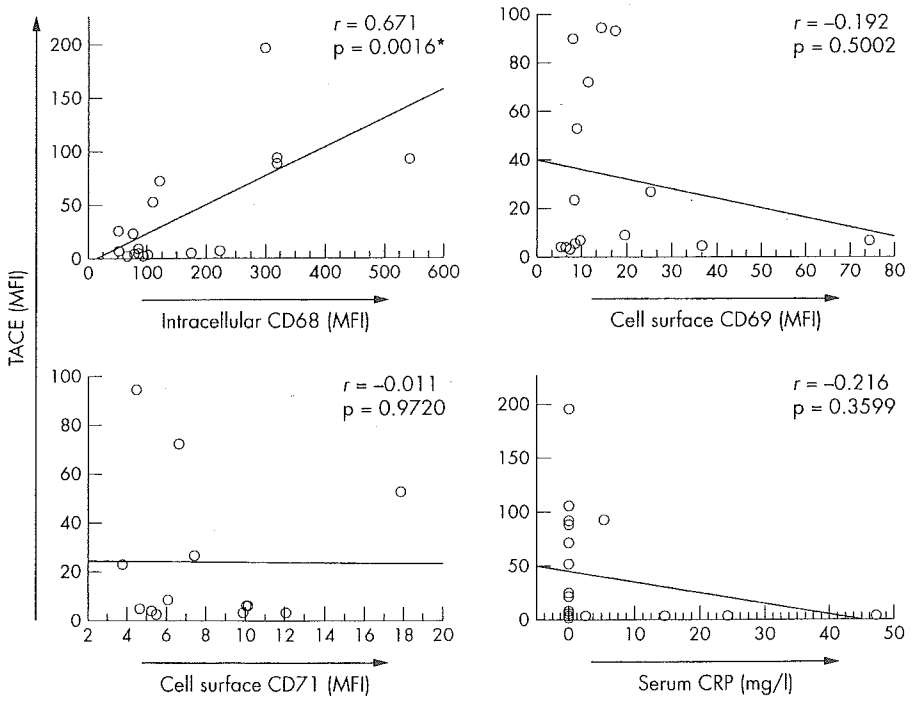


**Figure 5** Correlation of TACE protein expression levels and maturation/activation markers on monocytes, and serum CRP levels in patients with SSc. Correlation of TACE protein levels with intracellular CD68 expression, cell surface CD69 expression, cell surface CD71 expression, and serum C reactive protein (CRP) levels are displayed. Cells were stained with anti-TACE-PE monoclonal antibody, or with FITC-anti-CD68, CD69, and CD71, in the presence of anti-CD14-FITC. Intracellular or cell surface levels of each marker were measured by FACS, gating on the monocytes as described above. The expression levels of individual proteins, represented by the MFI, were plotted on the horizontal axis (CD68, CD69, and CD71) and on the vertical axis (TACE), respectively. Serum CRP levels were measured by a latex agglutination test. *$p<0.05$.

evidence of disease-specific up regulation of TACE in peripheral monocytes in SSc, both at mRNA and protein expression levels.

TACE is a metalloproteinase of the ADAM (a disintegrin and metalloproteinase) family, and was initially described as a protease responsible for processing the membrane anchored TNFα precursor to the mature secreted form.[36 37] It is now accepted that substrates of TACE also include various cell surface proteins other than pro-TNFα; TNF receptors type I (TNF-RI) and type II (TNF-RII), L-selectin, IL6 receptor α chain, TNF related activation induced cytokine, and fractalkine (reviewed by Mezyk *et al*[41]). TACE mRNA is expressed by various types of cells, and can be induced by various extracellular stimuli.[41 42] We found that expression of TACE increased at mRNA levels in PBMC from patients with SSc (table 3, fig 1). Moreover, expression levels of TACE protein correlated with that of intracellular CD68, a lysosomal antigen expressed during differentiation of monocytes to macrophages, and did not correlate with CD69, CD71, activation markers in blood cell, and CRP levels (fig 5).[43] In patients with RA with positive CRP, surface TACE protein levels in peripheral monocytes also had no correlation ($r = -0.277$, $p = 0.1459$). Monocytes from patients with early stage SSc were likely to be activated in vivo, expressing TACE, independently of general acute reactants. Expression of TACE mRNA is regulated by transcription factors, including AP-2 and SP-1.[44] Analysis of these factors may help in understanding the mechanism of TACE up regulation.

It was notable that TACE up regulation in monocytes was not seen in patients with chronic SSc with diffuse skin sclerosis (fig 4). Hence, up regulation of TACE in circulating monocytes was probably not a secondary outcome from a persistent fibrotic condition. In the pathogenesis of SSc, TGFβ and connective tissue growth factor (CTGF) dysfunction has been considered.[8 45] In addition, the up regulated TNFα/TNF-R system has also been suggested in recent studies. It has been reported that the serum soluble TNF-R levels significantly correlated with the activity and disease progression of SSc.[46 47] Furthermore, Ellman and MacDonald reported a significant improvement in the skin score of patients with SSc after administration of recombinant anti-TNFα antibody.[48] These findings are consistent with involvement of an aberrant function of the TNFα/TNF-R system in SSc. The up regulation of TACE may be involved in such abnormality in TNF signalling in SSc through the cleaving function of TACE.

The effect of TACE on the function of the TNFα/TNF-R system in vivo is not fully understood, but the soluble form of TNFα can interact with both TNF-RI and TNF-RII.[49–51] Ligation of TNF-RI leads to recruitment of intracellular signalling proteins, resulting in the bifurcation of TNF-RI signalling: one is the apoptotic signal delivered through caspase-8, and the other is activation of proinflammatory properties delivered through nuclear factor-κB (NF-κB) inducing kinase (NIK) and NF-κB.[52] Unlike TNF-RI, signalling through TNF-RII largely leads to activation of NIK dependent and NF-κB dependent signalling.[53] Thus, increased activity of TACE can shift the balance of signals mediated by distinct types of TNF receptors and downstream events, including activation or death of target cells. Interestingly, mice with a targeted mutation in TACE were perinatally lethal and had morphological defects in the skin, indicating the essential role of TACE in normal skin development.[54]

Thus, it is intriguing to consider that TACE may participate in the progression of skin involvement in SSc, especially at the early stage. However, TNFα can also down regulate the expression of CTGF and indirectly modulate expression of type II TGFβ receptor in human fibroblasts.[55 56] In addition, TACE can also cleave other functional molecules as well as TNFα and the receptors.[41] Such pleiotrophic action of TACE makes it difficult to predict a bona fide role of TACE up regulation in SSc. Further investigation of the function of TACE, including analysis of laboratory animals that overexpress TACE, may provide information about the significance of TACE in SSc.

In summary, this study described for the first time the aberrant expression of TACE on monocytes from patients with early SSc. Recently, several chemical compounds have been reported to inhibit the activities of metalloproteinases, including TACE.[57] Such reagents may have a role in cases of TACE associated chronic inflammatory disease, including SSc. In addition, expression of TACE levels may also be a useful clinical measure of SSc, reflecting disease stages and the clinical prognosis of individual patients. Analysis of TACE function in SSc monocytes may not only provide insight into the pathogenesis but may also be a new diagnostic and therapeutic target for SSc.

## ACKNOWLEDGEMENTS

We thank Ms Akiko Hirano for expert technical assistance, Drs Hiroshi Kataoka, Akira Furusaki, Katsuya Fujimoto, and Tomoyuki Endo for clinical procedures related to HSCT.
This work was supported by a national grant aid (14570004) from the Ministry of Education, Science, Technology, Sports, and Culture of Japan and a research grant for the study of the action of short fatty chain acid on cytokine gene regulation.

## Authors' affiliations

**T Bohgaki, Y Amasaki, M Bohgaki, Y Yamashita, M Nishio, S Jodo, T Atsumi, T Koike,** Department of Medicine II, Hokkaido University Graduate School of Medicine, N-15 W-7, Kita-ku, Sapporo 060-8638, Japan
**N Nishimura,** GeneticLab Co, Ltd, N-27 W-6, Kita-ku, Sapporo 001-0027, Japan
**K-i Sawada,** Department of Internal Medicine III, Akita University School of Medicine, 1-1-1 Hondo, Akita 010-8543, Japan

## REFERENCES

1 **Wigley FM**, Hummers LK. Systemic sclerosis. In: Hochberg MC, Silman AJ, Smolen JS, Weinblatt ME, Weisman MH, eds. *Rheumatology*.3rd ed. Edinburgh, UK: Mosby, 2003:1455–522.
2 **Furst DE**, Clements PJ. Hypothesis for the pathogenesis of systemic sclerosis. *J Rheumatol* 1997;**24**(suppl 48):53–7.
3 **Sakkas LI**, Platsoucas CD. Is systemic sclerosis an antigen-driven T cell disease? *Arthritis Rheum* 2004;**50**:1721–33.
4 **Sakkas LI**, Xu B, Artlett CM, Lu S, Jimenez SA, Platsoucas CD. Oligoclonal T cell expansion in the skin of patients with systemic sclerosis. *J Immunol* 2002;**168**:3649–59.
5 **Saito E**, Fujimoto M, Hasegawa M, Komura K, Hamaguchi Y, Kaburagi Y, *et al*. CD19-dependent B lymphocyte signalling thresholds influence skin fibrosis and autoimmunity in the tight-skin mouse. *J Clin Invest* 2002;**109**:1453–62.
6 **Varga J**. Scleroderma and Smads: dysfunctional Smad family dynamics culminating in fibrosis. *Arthritis Rheum* 2002;**46**:1703–13.
7 **Zhou X**, Tan FK, Xiong M, Milewicz DM, Feghali CA, Fritzler MJ, *et al*. Systemic sclerosis (scleroderma): specific autoantigen genes are selectively overexpressed in scleroderma fibroblasts. *J Immunol* 2001;**167**:7126–33.
8 **Luzina IG**, Atamas SP, Wise R, Wigley FM, Choi J, Xiao HQ, *et al*. Occurrence of an activated, profibrotic pattern of gene expression in lung CD8+T cells from scleroderma patients. *Arthritis Rheum* 2003;**48**:2262–74.
9 **Burt RK**, Traynor AE, Craig R, Marmont AM. The promise of haematopoietic stem cell transplantation for autoimmune diseases. *Bone Marrow Transplant* 2003;**31**:521–4.
10 **Tyndall A**, Passweg J, Gratwohl A. Haematopoietic stem cell transplantation in the treatment of severe autoimmune diseases 2000. *Ann Rheum Dis* 2001;**60**:702–7.
11 **Binks M**, Passweg JR, Frust D, McSweeney P, Sullivan K, Besenthal C, *et al*. Phase I/II trial of autologous stem cell transplantation in systemic sclerosis: procedure related mortality and impact on skin disease. *Ann Rheum Dis* 2001;**60**:577–84.
12 **Tyndall A**, Koike T. High-dose immunoablative therapy with haematopoietic stem cell support in the treatment of severe autoimmune disease: current status and future direction. *Intern Med* 2002;**41**:608–12.
13 **Farge D**, Passweg J, van Laar JM, Marjanovic Z, Besenthal C, Finke J, *et al*. Autologous stem cell transplantation in the treatment of systemic sclerosis: report from the EBMT/EULAR registry. *Ann Rheum Dis* 2004;**63**:974–81.
14 **ARA**. Preliminary criteria for the classification of systemic sclerosis (scleroderma). Subcommittee for scleroderma criteria of the American

Rheumatism Association Diagnostic and Therapeutic Criteria Committee. *Arthritis Rheum* 1980;**23**:581–90.
15 **LeRoy EC**, Krieg T, Black C, Jablonska S, Krieg T, Medsger TA Jr, *et al.* Scleroderma (systemic sclerosis); classification, subsets and pathogenesis. *J Rheumatol* 1988;**15**:202–5.
16 **Arnett FC**, Edworthy SM, Bloch DA, McShane DJ, Fries JF, Cooper NS, *et al.* The American Rheumatism Association 1987 revised criteria for the classification of rheumatoid arthritis. *Arthritis Rheum* 1998;**31**:315–24.
17 **Hochberg MC**. Updating the American College of Rheumatology revised criteria for the classification of systemic lupus erythematosus. *Arthritis Rheum* 1997;**40**:1725.
18 **Warrick JH**, Bhalla M, Schabel SI, Silver RM. High resolution computed tomography in early scleroderma lung disease. *J Rheumatol* 1991;**18**:1520–8.
19 **Clements PJ**, Furst DE, Campion DS, Bohan A, Harris R, Levy J, *et al.* Muscle disease in progressive systemic sclerosis: diagnostic and therapeutic considerations. *Arthritis Rheum* 1978;**21**:62–71.
20 **Della Rossa A**, Valentini G, Bombardieri S, Bencivelli W, Silman AJ, D'Angelo S, *et al.* European multicentre study to define disease activity criteria for systemic sclerosis. I. Clinical and epidemiological features of 290 patients from 19 centres. *Ann Rheum Dis* 2001;**60**:585–91.
21 **Steen VD**. Scleroderma renal crisis. *Rheum Dis Clin North Am* 1996;**22**:861–78.
22 **Roberts NK**, Cabeen WR, Moss J, Clements PJ, Furst DE. The prevalence of conduction defects and cardiac arrhythmias in progressive systemic sclerosis. *Ann Intern Med* 1981;**94**:38–40.
23 **Nagasako T**, Sugiyama T, Mizushima T, Miura Y, Kato M, Asaka M. Up-regulated Smad5 mediates apoptosis of gastric epithelial cells induced by Helicobactor pylori infection. *J Biol Chem* 2003;**278**:4821–5.
24 **Contin C**, Pitard V, Itai T, Nagata S, Moreau JF, Dechanet-Merville J. Membrane-anchored CD40 is processed by the tumour necrosis factor-α-converting enzyme. *J Biol Chem* 2003;**278**:32801–9.
25 **Atamas SP**, White B. The role of chemokines in the pathogenesis of scleroderma. *Curr Opin Rheumatol* 2003;**15**:772–7.
26 **LeRoy EC**, Mercurio S, Sherer GK. Replication and phenotypic expression of control and scleroderma human fibroblasts: responses to growth factors. *Proc Natl Acad Sci USA* 1982;**79**:1286–90.
27 **Prescott RJ**, Freemont AJ, Jones CJP, Hoyland J, Fielding P. Sequential dermal microvascular and perivascular changes in the development of scleroderma. *J Pathol* 1992;**166**:255–63.
28 **Kräling BM**, Maul GG, Jimenez SA. Mononuclear cellular infiltrates in clinically involved skin from patients with systemic sclerosis of recent onset predominantly consist of monocytes/macrophages. *Pathobiology* 1995;**63**:48–56.
29 **Tamby MC**, Chanseaud Y, Guillevin L, Mouthon L. New insights into the pathogenesis of systemic sclerosis. *Autoimmun Rev* 2003;**2**:152–7.
30 **Galindo M**, Santiago B, Rivero M, Rullas J, Alcami J, Pablos JL. Chemokine expression by systemic sclerosis fibroblasts: abnormal regulation of monocyte chemoattractant protein 1 expression. *Arthritis Rheum* 2001;**44**:1382–6.
31 **Bolster MB**, Ludwicka A, Sutherland SE, Strange C, Silver RM. Cytokine concentrations in bronchoalveolar lavage fluid of patients with systemic sclerosis. *Arthritis Rheum* 1997;**40**:743–51.
32 **Anderegg U**, Saalbach A, Haustein UF. Chemokine release from activated human dermal microvascular endothelial cells—implications for the pathophysiology of scleroderma? *Arch Dermatol Res* 2000;**292**:341–7.
33 **Minty A**, Chalon P, Guillemot JC, Kaghad M, Liauzun P, Magazin M, *et al.* Molecular cloning of the MCP-3 chemokine gene and regulation of its expression. *Eur Cytokine Netw* 1993;**4**:99–110.
34 **Ong VH**, Evans LA, Shiwen X, Fisher IB, Rajkumar V, Abraham DJ, *et al.* Monocyte chemoattractant protein 3 as a mediator of fibrosis. Over expression in systemic sclerosis and type 1 tight-skin mouse. *Arthritis Rheum* 2003;**48**:1979–91.
35 **Schmuth M**, Neyer S, Rainer C, Grassegger A, Fritsch P, Romani N, *et al.* Expression of the C-C chemokine MIP-3α/CCL20 in human epidermis with impaired permeability barrier function. *Exp Dermatol* 2002;**11**:135–42.
36 **Black RA**, Rauch CT, Kozlosky CJ, Peschon JJ, Slack JL, Wolfson MF, *et al.* A metalloproteinase disintegrin that releases tumour-necrosis factor-α from cells. *Nature* 1997;**385**:729–33.
37 **Moss ML**, Jin SLC, Milla ME, Burkhart W, Carter HL, Chen WJ, *et al.* Cloning of a disintegrin metalloproteinase that processes precursor tumour-necrosis factor-α. *Nature* 1997;**385**:733–6.
38 **Ohta S**, Harigai M, Tanaka M, Kawaguchi Y, Sugiura T, Takagi K, *et al.* Tumour necrosis factor-α (TNF-α) converting enzyme contributes to production of TNF-α in synovial tissues from patients with rheumatoid arthritis. *J Rheumatol* 2001;**28**:1756–63.
39 **Patel IR**, Attur MG, Patel RN, Stuchin SA, Abagyan RA, Abramson SB, *et al.* TNF-α convertase enzyme from human arthritis-affected cartilage: isolation of cDNA by differential display, expression of the active enzyme, and regulation of TNF-α. *J Immunol* 1998;**160**:4570–9.
40 **Seifert T**, Kieseier BC, Ropele S, Strasser-Fuchs S, Quehenberger F, Fazekas F, *et al.* TACE mRNA expression in peripheral mononuclear cells precedes new lesions on MRI in multiple sclerosis. *Mult Scler* 2002;**8**:447–51.
41 **Mezyk R**, Bzowska M, Bereta J. Structure and functions of tumour necrosis factor-α converting enzyme. *Acta Biochim Pol* 2003;**50**:625–45.
42 **Ermert M**, Pantazis C, Duncker HD, Grimminger F, Seeger W, Ermert L. In situ localization of TNF-α/β, TACE and TNF-receptors TNF-R1 and TNF-R2 in control and LPS-treated lung tissue. *Cytokine* 2003;**22**:89–100.
43 **Allavena P**, Piemonti L, Longoni D, Bernasconi S, Stoppacciaro A, Ruco L, *et al.* IL-10 prevents the differentiation of monocytes to dendritic cells but promotes their maturation to macrophages. *Eur J Immunol* 1998;**28**:359–69.
44 **Mizui Y**, Yamazaki K, Sagane K, Tanaka I. cDNA cloning of mouse tumour necrosis factor-α converting enzyme (TACE) and partial analysis of its promoter. *Gene* 1999;**233**:67–74.
45 **Holmes A**, Abraham DJ, Sa S, Shi-wen X, Black CM, Leask A. CTGF and SMADS, maintenance of scleroderma phenotype is independent of SMAD signalling. *J Biol Chem* 2001;**276**:10594–691.
46 **Gruschwitz MS**, Vieth G. Up-regulation of class II major histocompatibility complex and intracellular adhesion molecule 1 expression on scleroderma fibroblasts and endothelial cells by interferon-γ and tumour necrosis factor α in the early disease stage. *Arthritis Rheum* 1997;**40**:540–50.
47 **Gruschwitz MS**, Albrecht M, Vieth G, Haustein U. In situ expression and serum levels of tumour necrosis factor-α receptors in patients with early stage of systemic sclerosis. *J Rheumatol* 1997;**24**:1936–43.
48 **Ellman M**, MacDonald PA. Etanercept as treatment for diffuse scleroderma: a pilot study [abstract]. *Arthritis Rheum* 2000;**43**(suppl 9):S392.
49 **Grell M**, Douni E, Wajant H, Löhden M, Clauss M, Maxeiner B, *et al.* The transmembrane form of tumour necrosis factor is the prime activating ligand of the 80 kDa tumour necrosis factor receptor. *Cell* 1995;**83**:793–802.
50 **Tartaglia LA**, Pennica D, Goeddel DV. Ligand passing: the 75-kDa tumour necrosis factor (TNF-) receptor recruits TNF- for signalling by the 55-kDa TNF-receptor. *J Biol Chem* 1993;**268**:18542–8.
51 **Grell M**, Wajant H, Zimmermann G, Scheurich P. The type 1 receptor (CD120a) is the high-affinity receptor for soluble tumour necrosis factor. *Proc Natl Acad Sci USA* 1998;**95**:570–5.
52 **Malinin NL**, Boldin MP, Kovalenko AV, Wallach D. MAP3K-related kinase involved in NF-κB induction by TNF, CD95 and IL-1. *Nature* 1997;**385**:540–4.
53 **Pimentel-Muinos FX**, Seed B. Regulated commitment of TNF-receptor signalling: a molecular switch for death or activation. *Immunity* 1999;**11**:783–93.
54 **Peschon JJ**, Slack JL, Reddy P, Stocking KL, Sunnarborg SW, Lee DC, *et al.* An essential role for ectodomain shedding in mammalian development. *Science* 1998;**282**:1281–4.
55 **Abraham DJ**, Shiwen X, Black CM, Sa S, Xu Y, Leask A. Tumour necrosis factor α suppresses the induction of connective tissue growth factor by transforming growth factor-β in normal and scleroderma fibroblasts. *J Biol Chem* 2000;**275**:15220–5.
56 **Yamane K**, Ihn H, Asano Y, Jinnin M, Tamaki K. Antagonistic effects of TNF-α on TGF-β signalling through down-regulation of TGF-β receptor type II in human dermal fibroblasts. *J Immunol* 2003;**171**:3855–62.
57 **Conway JG**, Andrews RC, Beaudet B, Bickett DM, Boncek V, Brodie TA, *et al.* Inhibition of tumour necrosis factor-α (TNF-α) production and arthritis in the rat by GW3333, a dual inhibitor of TNF-α-converting enzyme and matrix metalloproteinases. *J Pharmacol Exp Ther* 2001;**298**:900–8.

ARTHRITIS & RHEUMATISM
Vol. 52, No. 9, September 2005, pp 2697–2707
DOI 10.1002/art.21258


# Butyrate Suppresses Tumor Necrosis Factor α Production by Regulating Specific Messenger RNA Degradation Mediated Through a *cis*-Acting AU-Rich Element

Jun Fukae, Yoshiharu Amasaki, Yumi Yamashita, Toshiyuki Bohgaki, Shinsuke Yasuda, Satoshi Jodo, Tatsuya Atsumi, and Takao Koike

*Objective.* **To study the capacity of butyrate to inhibit production of tumor necrosis factor α (TNFα) in macrophage-like synoviocytes (MLS) from patients with rheumatoid arthritis (RA), in human peripheral monocytes, and in murine RAW264.7 macrophages.**

*Methods.* **The concentrations of TNFα in culture supernatants of these cells were measured using enzyme-linked immunosorbent assay. The expression levels of various messenger RNAs (mRNA), such as those for TNFα, the mRNA-binding protein TIS11B, and luciferase, were measured using real-time quantitative polymerase chain reaction. The in vitro effects of butyrate on transcriptional regulation were evaluated by transfection with various reporter plasmids in RAW264.7 macrophages. The effects of TIS11B on TNFα expression were examined using an overexpression model of TIS11B in RAW264.7 cells.**

*Results.* **Butyrate suppressed TNFα protein and mRNA production in MLS and monocytes, but paradoxically enhanced transactivation of the TNFα promoter. Expression of the AU-rich element (ARE)–binding protein TIS11B was up-regulated by butyrate. Induction of TNFα mRNA by lipopolysaccharide was significantly inhibited when TIS11B was overexpressed. Butyrate facilitated the degradation of luciferase transcripts containing the 3′-untranslated region (3′-UTR) of TNFα, and this effect was dependent on the ARE in the 3′-UTR that is known to be involved in the regulation of mRNA degradation.**

*Conclusion.* **These results indicate that butyrate suppresses TNFα expression by facilitating mRNA degradation mediated through a *cis*-acting ARE. Butyrate has the ability to regulate TNFα at the mRNA level and is therefore a potential therapeutic drug for RA patients.**

Rheumatoid arthritis (RA) is a chronic inflammatory disease characterized by cartilage destruction and extracellular matrix degradation in multiple joints (1). The pathogenesis of RA is not clearly understood; however, tumor necrosis factor α (TNFα) is involved in its development, a conclusion which is supported by successful treatments with anti-TNFα reagents (2). The production of TNFα was found to be increased in rheumatoid synovium, followed by the induction of other proinflammatory cytokines, including interleukin-1β (IL-1β), IL-6, and IL-8, as well as matrix metalloproteinases involved in cartilage and bone destruction in RA (3–5). These cytokines are involved in synovial cell activation and proliferation, leading to generation of pannus (6).

Synovial tissue consists of heterogeneous immune and non–immune cell populations, including fibroblast-like synoviocytes, macrophage-like synoviocytes (MLS), lymphocytes, dendritic cells, and endothelial cells (7). Among these populations, MLS originating from bone marrow–derived monocytes are largely responsible, upon activation, for the production of TNFα protein (6). Monocytes can give rise to osteoclasts involved in rheumatoid bone destruction (8). The mech-

Supported by the Ministry of Education, Science, Technology, Sports, and Culture of Japan (grant 14570004) and by a research grant for study of the action of short chain fatty acids on cytokine gene regulation.

Jun Fukae, MD, PhD, Yoshiharu Amasaki, MD, PhD, Yumi Yamashita, PhD, Toshiyuki Bohgaki, MD, PhD, Shinsuke Yasuda, MD, PhD, Satoshi Jodo, MD, PhD, Tatsuya Atsumi, MD, PhD, Takao Koike, MD, PhD: Hokkaido University Graduate School of Medicine, Sapporo, Japan.

Address correspondence and reprint requests to Yoshiharu Amasaki, MD, Department of Medicine II, Hokkaido University Graduate School of Medicine, Kita-15, Nishi-7, Kita-ku, Sapporo 060-8638, Japan. E-mail: yamasaki@med.hokudai.ac.jp.

Submitted for publication December 6, 2004; accepted in revised form June 3, 2005.

anisms of MLS activation have been only partially understood. Macrophages express TNFα via activation of Toll-like receptor 4–NF-κB signaling, and this type of activation may be mimicked experimentally by administration of lipopolysaccharide (LPS) (9,10).

TNFα-mediated chronic inflammation has also been studied in inflammatory bowel diseases and in animal models of such diseases. In those studies, physiologic roles for short-chain fatty acids have been identified (11,12). Short-chain fatty acids are a natural product of colonic anaerobic fermentation of dietary fiber by luminal microflora. These are the preferred sources of energy for the normal colonic epithelial cell, and they can modulate a variety of fundamental cellular processes to induce cell-cycle arrest, differentiation, and apoptosis in transformed cells (13,14). These molecules, especially butyrate, have potent antiinflammatory effects and can modulate TNFα expression in colonic epithelial cells and in monocytes (15). It has also been shown that administration of butyrate suppresses experimental enteritis induced in mice by dextran sulfate sodium (16). Experiments in colonocytes revealed that butyrate down-regulates TNFα expression by modulating NF-κB–DNA binding activity (15), although the precise mechanism is not fully understood. In addition, butyrate is known to function as a histone deacetylase (HDA) inhibitor in cells, and it can induce alteration of the chromatin structure (17,18), although the effect of this activity on TNFα down-regulation is not yet understood. We investigated whether butyrate could suppress TNFα production in activated synovial cells and macrophages, in order to evaluate short-chain fatty acids as a potential investigational new treatment for chronic inflammation in RA.

## MATERIALS AND METHODS

**Preparation of primary synoviocytes and culture.** Primary synoviocytes were obtained from surgically resected synovial tissue from Japanese patients with RA. Informed consent was obtained from each patient. Tissue specimens were minced and dissociated in Hanks' balanced salt solution (Invitrogen, Carlsbad, CA) containing 5 mg/ml type I collagenase (Sigma, St. Louis, MO) and 0.15 mg/ml DNase I (Sigma) for 2 hours at 37°C. Samples were then passed through a metal mesh and a nylon mesh, each with a 100-μm pore size. Cells were collected by centrifugation and resuspended at $0.5 \times 10^6$/ml in Iscove's modified Dulbecco's medium (Invitrogen) containing 10% heat-inactivated fetal bovine serum (FBS) and antibiotics. The resulting synoviocytes were cultured in a 6-well tissue culture plate (Becton Dickinson, Mountain View, CA) at 37°C in a humidified atmosphere with 5% $CO_2$ for 24–48 hours. Our primarily rheumatoid synoviocyte cultures contained ~10–35% of a CD14-positive subpopulation as assessed by fluorescence-activated cell sorting (FACS Calibur system; Becton Dickinson) (data not shown). The proportion of CD14-positive rheumatoid synoviocytes varied depending on the patient's background, such as duration or activity of the disease and treatment. Before the stimulation assay, nonadherent cells were removed by washing twice with phosphate buffered saline (PBS).

**Cell culture and stimulation.** Human monocytes were enriched from whole blood obtained from healthy Japanese volunteers. The mononuclear cell fraction was prepared by density-gradient centrifugation over Ficoll-Paque (Amersham Biosciences, Uppsala, Sweden), followed by plating in culture medium at 37°C for 1 hour in a humidified incubator to obtain the adherent cells. After washing the cells twice with PBS, adherent cells were resuspended in RPMI 1640 medium (Invitrogen) containing 10% heat-inactivated FBS and antibiotics, then counted and diluted to $0.5 \times 10^6$/ml. Cells were processed for the stimulation assay on the same day that the blood was collected. Purity of CD14-positive cells was 80–90% as assessed by fluorescence-activated cell sorting (data not shown). The murine macrophage cell line RAW264.7 (no. TIB-71; American Type Culture Collection, Rockville, MD) was grown in Dulbecco's modified Eagle's medium (DMEM; Invitrogen) containing 10% heat-inactivated FBS and antibiotics at 37°C in a humidified atmosphere with 5% $CO_2$ (19). Cells were resuspended at $0.25 \times 10^6$/ml, then 2 ml/well of the cell suspension was transferred to 6-well tissue culture plates, followed by 24 hours of culture before stimulation. After preincubation, cells were stimulated with LPS (no. L4391; Sigma) or were used without stimulation. In some experiments, various concentrations of sodium butyrate (Sigma) were included in the culture. Where indicated, actinomycin D (Sigma) was also included in the culture to restrict transcriptional events.

**RNA preparation and real-time quantitative polymerase chain reaction (PCR) analysis.** Total RNA was obtained by using TRIzol RNA Reagent (Invitrogen) according to the manufacturer's instructions. In some experiments, total RNA was extracted from transfected cells using the Concert Cytoplasmic RNA Reagent (Invitrogen) in combination with DNase I Amplification Grade (Invitrogen) to eliminate residual plasmid DNA. RNA samples were reverse-transcribed using oligo(dT) primers and ReverTra Ace (Toyobo, Osaka, Japan) according to the manufacturer's instructions. Real-time quantitative PCR analyses were performed using 100 n*M* TaqMan probe and 200 n*M* forward and reverse primers in a final volume of 30 μl using 2×PCR reagent (Applied Biosystems, Chiba, Japan) in an ABI PRISM 7000 Sequence Detection System instrument (Applied Biosystems) based on dual-labeled fluorogenic probe technology (20).

The following forward and reverse primers and TaqMan probes, designed by Primer Express software (Applied Biosystems), were used for analyses: mouse TNFα, forward primer 5′-CAGACCCTCACACTCAGATCATCT-3′, reverse primer 5′-GCACCACTAGTTGGTTGTCTTTGA-3′, TaqMan probe 5′-CAAGCCTGTAGCCCACGTCGTAGCA-3′; mouse TIS11B, forward primer 5′-TTGTTGGTAGCTTCTGGCTTGA-3′, reverse primer 5′-GGCATCTACTGACAAAAGATGGAA-3′, TaqMan probe 5′-TCCATTTCATAGCCCACTTAACCACGCA-3′; luciferase, forward primer 5′-TGACCGCCTGAAGTCTCTGA-3′, reverse primer 5′-

ACACCTGCGTCGAAGATGTTG-3′, TaqMan probe 5′-CCGCTGAATTGGAATCCATCTTGCTC-3′; AU-rich element (ARE) mutation, forward primer 5′-ATGCACAG-CCTTCCTCACAG-3′, reverse primer 5′-CCCGGCCT-TCCAAATAAATAC-3′, minor groove binder (MGB) TaqMan probe 5′-TATCCATTATCCATCCATTATCCATC-3′. The first 3 TaqMan probes were labeled on the 5′ end with FAM reporter dye and on the 3′ end with TAMRA quencher dye; the ARE mutation MGB TaqMan probe was labeled on the 5′ end with FAM reporter dye and on the 3′ end with conjugated MGB.

To measure the gene copy number of the various transcripts, the purified artificial gene product containing an amplification sequence was serially diluted to achieve a standard curve. Data for each messenger RNA (mRNA) quantity were normalized based on the mRNA copy number of GAPDH obtained using the TaqMan rodent GAPDH control reagents (Applied Biosystems).

**Enzyme-linked immunosorbent assay (ELISA).** The concentrations of human and mouse TNFα proteins were determined using specific sandwich ELISA kits (no. 656227 from Cosmo Bio [Tokyo, Japan] and no. 10019 from Genzyme [Cambridge, MA], respectively) according to the manufacturers' instructions.

**Plasmid construction.** The luciferase reporter plasmids pNFκB-Luc and pGL3-BASIC were purchased from Stratagene (La Jolla, CA) and Promega (Madison, WI), respectively. Murine genomic DNA extracted from a normal C57BL/6 mouse using a standard protocol (21) was used for amplification of a genomic DNA fragment of the mouse TNFα gene. A 0.9-kb DNA fragment corresponding to the 5′-untranslated region (5′-UTR) of the mouse TNFα gene was PCR-amplified with the sense and antisense primers 5′-CTC-AAGCTTATCAGAGTGAAAGGAGAAGGC-3′ and 5′-CTCAAGCTTAGTGAAAGGGACAGAACCTGC-3′, respectively. The product was inserted into the *Hind* III cloning site of pGL3-BASIC and designated pGL-mTNFα. The 0.8-kb 3′-UTR of the mouse TNFα gene was similarly amplified using PCR, and the *Xba* I and *Bam* HI restriction sites were introduced with the PCR primers 5′-TCTAGAGGGAATGGG-TGTTCATCC-3′ and 5′-GGATCCCATGCCCCAGGGCAAA-3′, respectively. The resulting DNA fragment was used to replace the 3′-UTR of the pGL-mTNFα, and the resulting plasmid was designated pGL-mTNFα-UTR.

A pGL-CMV-UTR plasmid, in which the luciferase gene was constitutively expressed under the control of the cytomegalovirus (CMV) promoter, was generated by replacing the *Hind* III fragment corresponding to the TNFα promoter region in the pGL-mTNFα-UTR vector with a DNA fragment containing the CMV promoter sequences from pFLAG-CMV-2 (Sigma). In addition, the AT repeat (ARE) in pGL-CMV-UTR corresponding to the TNFα 3′-UTR sequence (+1299 to +1332) was mutated to yield an ARE mutation plasmid (pGL-CMV-UTR/mARE) using standard recombinant techniques and the mutagenic oligonucleotide 5′-ACAGCCTTCCTCACAGAGCCAGCCCCCCTCTATT-TATATTTGCACTTATTATCCATTATCCATCCATTAT-CCATCCATTTGCTTATGAATGTATTTATTTGGAAG-GCCG-3′. The sequences of all the DNA fragments obtained by PCR amplification were confirmed by DNA sequencing and completely matched the reported mouse TNFα genomic sequence (GenBank accession no. Y00467) (22).

A mammalian expression plasmid, pFLAG-TIS11B, that encodes mouse TIS11B complementary DNA (cDNA) (23) was generated by introducing a mouse full-length TIS11B cDNA fragment into the pFLAG-CMV-2 plasmid (Sigma). The TIS11B cDNA fragment was obtained by PCR amplification of cDNA from RAW264.7 cells and the specific sense and antisense primers 5′-GAATTCGATGACCACCACCCTCGT-3′ and 5′-TCTAGAGGAGAGGTGAAGGAGGCATG-3′, respectively. After subcloning into pCR-blunt and confirmation by DNA sequencing, the 1.2-kb fragment corresponding to the TIS11B cDNA (GenBank accession no. BC016621) was excised and ligated into pFLAG-CMV-2 at the *Xba* I and *Eco* RI cloning sites.

**Transfection and luciferase assay.** RAW264.7 cells ($0.25 \times 10^5$) were transferred to 8-cm tissue culture plates (Becton Dickinson) and incubated for 24 hours to 70% confluence. Transfections were achieved using Transfectam reagent (Promega), according to the manufacturer's instructions, with the plasmids described above. Plasmid DNA (10 μg) was mixed with 20 μl of Transfectam reagent in 3 ml of FBS-free DMEM and transferred to the plates. After 2 hours of incubation, complete culture medium was added to the cells, followed by further incubation to semiconfluence. The transfection efficiency in the current protocol was ~5% when cells transfected with green fluorescent protein–expressing plasmid were analyzed by fluorescence-activated cell sorting (data not shown). Transfected cells were collected and distributed into new 6-well tissue culture plates (Becton Dickinson) before the stimulation assay. This step was performed to equalize the number of transfected cells and eliminate any differences in transfection efficiency between plates.

Where indicated, the luciferase assay was carried out according to the procedure described previously with minimal modifications (24). Briefly, RAW264.7 cells were transfected with various reporter plasmids as described above. After incubation and stimulation, cells were lysed using lysis buffer (Promega). Cell lysates were stored at −80°C until the luciferase assay was performed. The protein content of each sample was determined using a protein assay reagent (Bio-Rad, Hercules, CA), and the luciferase activities of the samples were normalized according to the protein content of the samples. Data are reported as relative luciferase units.

**Cell proliferation assay.** In order to exclude the possibility that butyrate directly affects cell viability, a proliferation assay was performed using MTS (3-(4,5-dimethylthiazol-2-yl)-5-(3-carboxymethoxyphenyl)-2-(4-sulfophenyl)-2H-tetrazolium) tetrazolium assay (Cell Titer96 AQueous One Solution Cell Proliferation Assay; Promega). RAW264.7 cells ($0.25 \times 10^5$) were transferred into microtiter-plate wells in 100 μl of DMEM containing various concentrations of butyrate, then MTS reagent was added to the wells. Optical density was read using a microplate autoreader (Microplate Reader Model 3550; Bio-Rad) at a wavelength of 490 nm after addition of MTS reagent.

**Statistical analysis.** Statistical analyses were calculated by Student's *t*-test with the use of the Excel program (Microsoft, Redmond, WA).

## RESULTS

**Suppression by butyrate of TNFα protein production in cultured primary synoviocytes.** We first analyzed the effect of butyrate on TNFα production in rheumatoid synoviocytes during stimulation with LPS. When primary synoviocytes were stimulated with LPS, significant amounts of TNFα protein were detected in the culture supernatants (Figure 1A). Addition of butyrate to the culture medium led to a significant, dose-dependent decrease in LPS-stimulated TNFα production. MLS, major producers of TNFα in the rheumatoid inflammatory synovium, play an important role in the initiation of synovitis and bone destruction (25). We paid attention to the subpopulation of monocyte/macrophages, and thus we repeated the experiments on the effect of butyrate on TNFα production both by peripheral monocytes and by the macrophage cell line RAW264.7. Human peripheral monocytes and RAW264.7 cells both secreted significant amounts of TNFα upon LPS stimulation (Figures 1B and C). As was the case in the primary cell culture, there was a significant decrease in LPS-stimulated TNFα secretion with increasing butyrate concentrations in the medium. In all experiments, similar GAPDH mRNA expression levels were confirmed in each cell preparation after treatment with LPS/butyrate (data not shown).

RAW264.7 cells were exposed to various concentrations of butyrate, and MTS tetrazolium assay was performed to assess cell proliferation. The results revealed that butyrate had no significant effect on cell proliferation (Figure 2B).

**Suppression by butyrate of TNFα expression at the mRNA level in monocytes and in the macrophage cell line RAW264.7.** To determine how butyrate regulates TNFα production in monocytes, we next examined the effect of butyrate on TNFα mRNA expression. We performed semiquantitative reverse transcriptase (RT)–PCR analysis using specific primers for initial screening and found that butyrate suppressed TNFα mRNA induction in response to stimulation with LPS in human monocytes (data not shown). Butyrate also suppressed LPS-stimulated TNFα production in RAW264.7 cells in a dose-dependent manner, confirmed by real-time quantitative PCR (Figure 2A). The macrophage cell line RAW264.7 is responsive to butyrate; therefore, we used the RAW264.7 cells as an appropriate system for transfection assay.

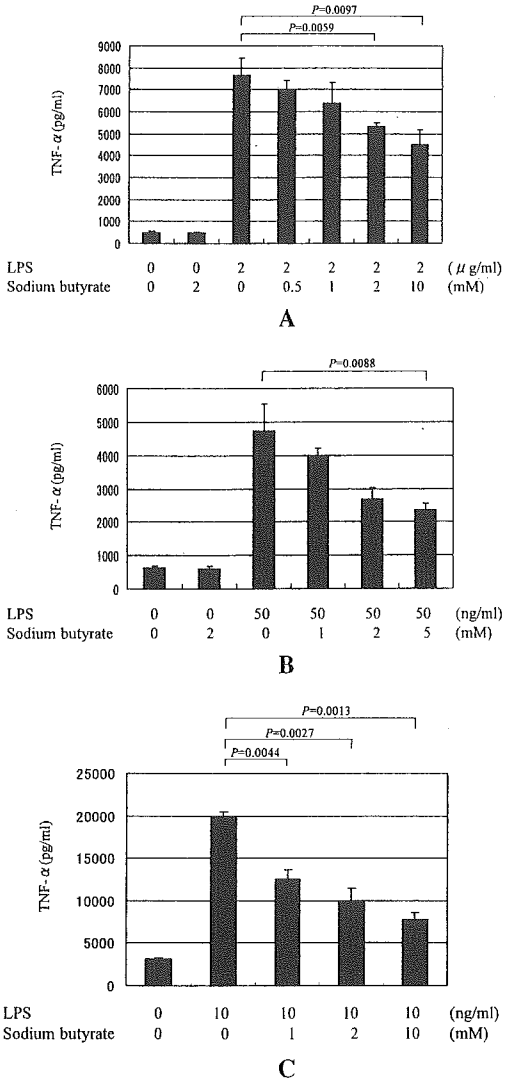


**Figure 1.** Effects of butyrate on tumor necrosis factor α (TNFα) protein secretion by synoviocytes and monocytes. An enzyme-linked immunosorbent assay (ELISA) specific for human TNFα protein was used to determine levels of TNFα in **A,** culture supernatants of primary synoviocytes (obtained from patients with rheumatoid arthritis) not stimulated with lipopolysaccharide (LPS) or stimulated with 2 μg/ml LPS for 6 hours in the presence or absence of sodium butyrate, and **B,** human peripheral blood monocytes (obtained from healthy donors) not stimulated with LPS or stimulated with 50 ng/ml LPS for 4 hours in the presence or absence of sodium butyrate. **C,** Levels of mouse TNFα were measured in culture supernatants from RAW264.7 cells not stimulated with LPS or stimulated with 10 ng/ml LPS for 6 hours in the presence or absence of sodium butyrate, using an ELISA specific for mouse TNFα. Experiments in **A, B,** and **C** were repeated 15, 9, and 6 independent times, respectively, and representative results are shown. Values are the mean and SEM.

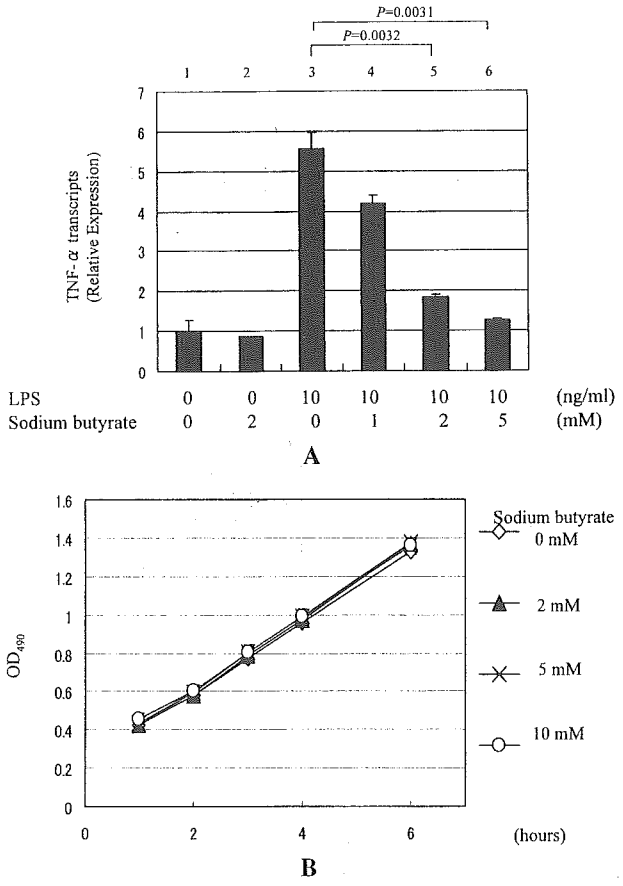


**Figure 2.** Effects of butyrate on TNFα mRNA expression and cell proliferation in RAW264.7 cells. **A,** Real-time quantitative polymerase chain reaction (PCR) (described in Materials and Methods) was used to estimate TNFα expression in RAW264.7 cells not stimulated with LPS (lanes 1 and 2) or stimulated with 10 ng/ml LPS (lanes 3–6) in the presence (lanes 2 and 4–6) or absence (lanes 1 and 3) of sodium butyrate for 2 hours. The amount of TNFα cDNA transcripts is displayed as a relative value obtained by dividing the value for TNFα transcripts by the value for GAPDH cDNA transcripts. Real-time quantitative PCR data were obtained from triplicate transwells and are representative of 3 independent experiments. Values are the mean and SEM. **B,** Cell proliferation assay (described in Materials and Methods) was used to examine the toxicity of butyrate on RAW264.7 cells. Cells were treated with various concentrations of butyrate (0, 2, 5, and 10 m*M*), and the optical density (OD) was read at a wavelength of 490 nm serially at 1-, 2-, 3-, 4-, and 6-hour time points. Data were obtained from triplicate transwells. Values are the mean ± SEM of 3 independent experiments. See Figure 1 for other definitions.

**No suppression by butyrate of transcriptional activity driven through the TNFα promoter.** To test whether butyrate could affect TNFα mRNA expression via transcriptional repression, RAW264.7 cells were transfected with reporter plasmids containing the consensus NF-κB binding sequence or the full-length TNFα promoter sequence. When cells were transfected with pNFκB-Luc or pGL-mTNFα, however, butyrate did not suppress the transcriptional activities (Figures 3A and B). Instead, butyrate showed a dose-dependent enhancement of transactivation, which was inconsistent with its effects on the mRNA and protein expression of TNFα. These results indicate that butyrate regulates TNFα mRNA levels via a mechanism other than transcriptional repression in RAW264.7 cells.

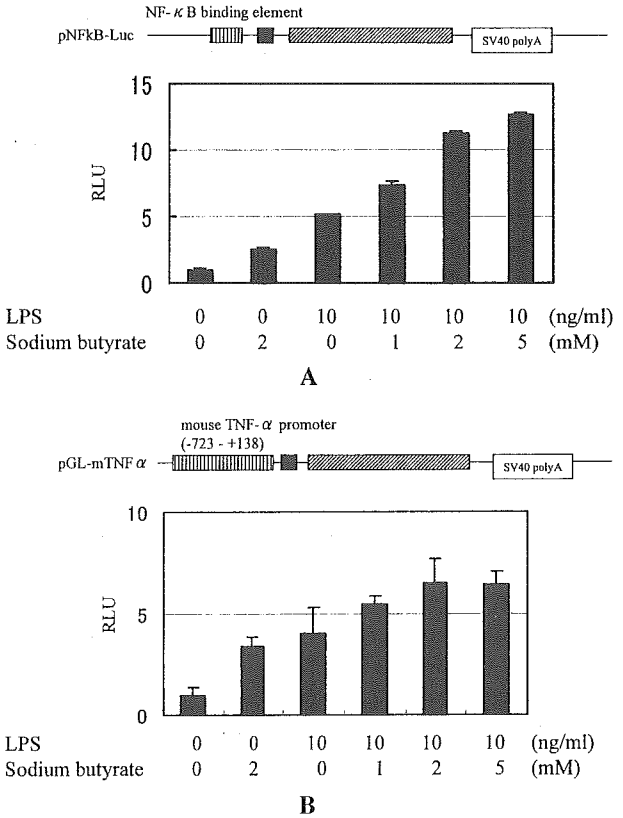


**Figure 3.** Effect of butyrate on TNFα promoter–related transcriptional activities. RAW264.7 cells were transfected with various types of luciferase reporter plasmids (see Materials and Methods for description of methods of transfection and luciferase assay). Forty-eight hours after transfection, cells were stimulated with 10 ng/ml LPS in the absence or presence of sodium butyrate (1, 2, or 5 m*M*) for 6 hours. The luciferase activities in cell lysates were measured and normalized using the protein concentration in each sample. **A,** Transcriptional activity of cells transfected with pNFκB-Luc. **B,** Transcriptional activity of cells transfected with pGL-mTNFα. Data shown in **A** and **B** were obtained from triplicate transwells and are representative of 6 independent experiments. Values are the mean and SEM. SV40 polyA = simian virus 40 late poly(A) signal; RLU = relative luciferase units (see Figure 1 for other definitions).

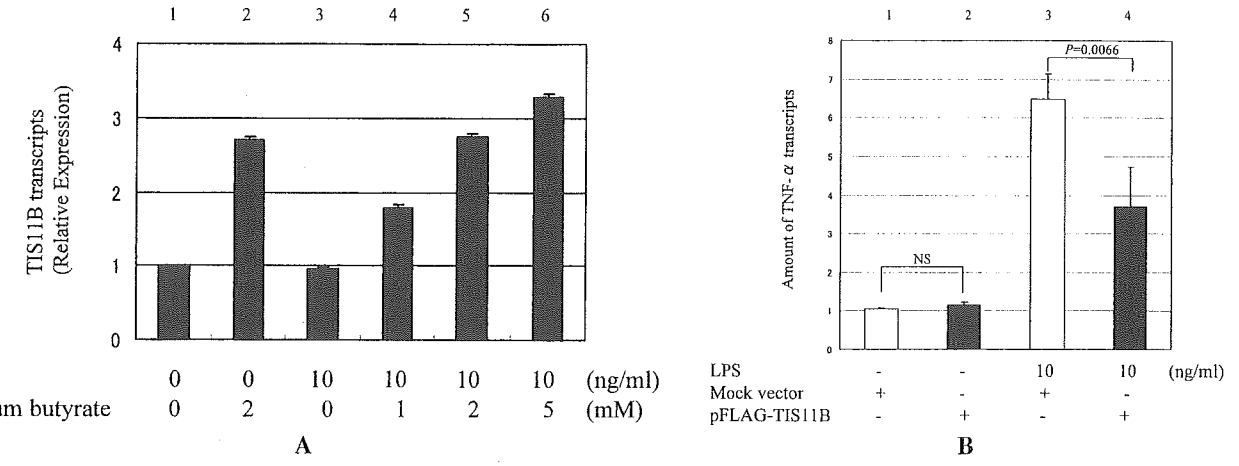


**Figure 4.** Expression of the tristetraprolin (TTP) family of genes in RAW264.7 cells upon treatment with butyrate. **A,** Expression of mRNA for TIS11B (a representative member of the TTP family of proteins) in RAW264.7 cells upon treatment with butyrate. RAW264.7 cells were not stimulated with LPS or were stimulated with 10 ng/ml LPS (lanes 3–6) in the presence (lanes 2 and 4–6) or absence (lanes 1 and 3) of butyrate. After 1 hour of stimulation, total RNA was obtained, followed by real-time quantitative polymerase chain reaction (PCR) for TIS11B. The amount of TIS11B cDNA transcripts is displayed as a relative value obtained by dividing the value for TIS11B transcripts by the value for GAPDH cDNA transcripts. Real-time quantitative PCR data were obtained from triplicate transwells and are representative of 3 independent experiments. Values are the mean and SEM. **B,** Effect of TIS11B on expression levels of TNFα mRNA in RAW264.7 cells stimulated with LPS. RAW264.7 cells were transfected with the TIS11B expression vector, pFLAG-TIS11B (solid bars) or with the control pFLAG empty (mock) vector (open bars). Forty-eight hours after transfection, cells were stimulated with 10 ng/ml LPS (lanes 3 and 4); total RNA was obtained after 2 hours of stimulation. The amount of TNFα cDNA transcripts was determined using real-time quantitative PCR. Data are schematically displayed as a relative value obtained by dividing the value for TNFα transcripts by the value for GAPDH cDNA transcripts. Real-time quantitative PCR data were obtained from triplicate transwells and are representative of 3 independent experiments. Values are the mean and SEM. NS = not significant (see Figure 1 for other definitions).

**TIS11B as a candidate molecule for butyrate-mediated inhibition of TNFα mRNA expression.** TNFα gene expression involves posttranscriptional regulation, including the ARE in the 3′-UTR that is thought to play a critical role in the regulatory mechanism (26). AREs are found in multiple cytokine genes including TNFα, and the *cis*-regulatory effects of these elements are mediated by several polypeptides that can bind AREs. Tristetraprolin (TTP) is an ARE-binding protein that facilitates TNFα mRNA degradation, and TIS11B and TIS11D are representative members of the TTP family of proteins that are also capable of interacting with AREs. We hypothesized that the effects of butyrate were related to the posttranscriptional regulation mediated through the AREs and ARE-binding proteins. To search for the butyrate-mediated induction of ARE-binding proteins, we first used semiquantitative RT-PCR to screen for the expression of TTP family proteins such as TTP, TIS11B, and TIS11D in RAW264.7 cells treated with butyrate. Among the factors examined, butyrate induced only TIS11B mRNA but neither TTP mRNA nor TIS11D mRNA (data not shown). Real-time quantitative PCR revealed that butyrate induced TIS11B mRNA in a dose-dependent manner (Figure 4A).

We determined that TIS11B had a suppressive effect on levels of TNFα mRNA. RAW264.7 cells were transfected with TIS11B expression plasmid or with a control mock vector, then stimulated with LPS. The expression level of TNFα mRNA decreased significantly in RAW264.7 cells transfected with TIS11B expression plasmid (Figure 4B). These results suggested that butyrate down-regulated levels of TNFα mRNA via binding of TIS11B to an ARE.

**Facilitation by butyrate of mRNA degradation via the function of an ARE in the TNFα 3′-UTR.** We next studied whether the inhibitory effects of butyrate on TNFα specifically depended on an ARE. To determine whether butyrate affects the amounts of gene transcripts carrying the TNFα 3′-UTR, we designed a real-time TaqMan RT-PCR–based quantitative assay that detects mRNA turnover (Figure 5). RAW264.7 cells were transfected with pGL-CMV-UTR reporter plasmid and treated with actinomycin D to repress generation of newly transcribed mRNA. To equalize the difference in transfection efficiency between plates, all transfected

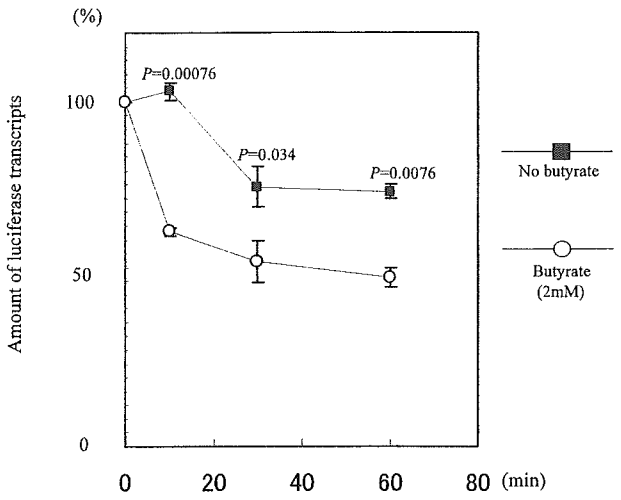


**Figure 5.** Effect of butyrate on the turnover of luciferase mRNA containing a tumor necrosis factor α 3′-untranslated region. RAW264.7 cells were transfected with pGL-CMV-UTR (see Materials and Methods). After no treatment or pretreatment with butyrate (2 m*M*) for 2 hours, cells were placed in culture medium containing actinomycin D (10 μg/ml) to halt transcription. Cells were then harvested serially at 0-, 10-, 30-, and 60-minute time points, and total RNA was extracted. After extensive treatment with RNase-free DNase I to digest the plasmid vector DNA, total RNA samples were reverse-transcribed for real-time quantitative polymerase chain reaction using primers specific for the luciferase gene product (described in Materials and Methods). The amount of luciferase cDNA transcripts is displayed as a relative value obtained by dividing the value for luciferase transcripts by the value for GAPDH cDNA transcripts. The datum at the 0-minute time point (for luciferase/GAPDH) was assigned a value of 100%, and other data are shown relative to this value. Values are the mean ± SEM of 3 independent experiments.

cells were collected and distributed into new plates before butyrate treatment. The time course of decrease of mRNA levels was in direct proportion to the rate of degradation. The amount of cDNA transcripts containing the 3′-UTR was serially quantified by real-time PCR. We observed a significant decrease in cDNA transcripts derived from pGL-CMV-UTR in cells treated with butyrate, both at the 10-minute time point and thereafter (Figure 5). This suggested that butyrate facilitated the degradation of mRNA transcripts of TNFα carrying the 3′-UTR sequence.

In various cytokine genes, including TNFα, an ARE in the 3′-UTR has been shown to affect stability of the gene transcripts (26). To test whether the inhibitory effects of butyrate on TNFα are mediated by the action of this *cis* ARE, we generated pGL-CMV-UTR/mARE containing a mutated ARE from pGL-CMV-UTR (Figure 6A). The amounts of transcripts derived from these plasmids were quantified and compared using RAW264.7 cells and the TaqMan PCR method. In this assay, total amounts of transcripts derived from mixed plasmids were determined by reactions using a luciferase TaqMan probe, and, at the same time, amounts of transcripts carrying the ARE mutation derived from these mixed plasmids were determined using an ARE mutation MGB TaqMan probe (Figure 6A). The quantification of these 2 transcripts was made possible by using a common gene standard, R-luc-AU, that contained both the mutated ARE and part of the common luciferase open reading frame sequence, and changes in the expression of these 2 transcripts were described as a ratio and calculated as follows: transcripts with mutated ARE:transcripts with intact ARE = (M/G):([A − M]/G) = M:(A − M), where A is the total amount of luciferase transcripts, M is the amount of transcripts with mutated ARE, and G is the internal control GAPDH.

As shown in Figure 6B, the amount of transcripts carrying mutated ARE and the amount carrying intact ARE were almost identical at the time point at which actinomycin D had stopped the transcription, when cells were treated (or not treated) with butyrate. It was shown that the relative amount of transcripts carrying a mutated ARE increased significantly during the time course. Thus, transcripts carrying the mutated ARE were more stable than those carrying intact ARE, and butyrate's ability to facilitate the degradation of transcripts was lost when the ARE was mutated. This indicates that the suppressive effect of butyrate on TNFα expression is mediated through the specific ARE in the 3′-UTR of the TNFα transcript.

## DISCUSSION

In this report, we have shown that butyrate strongly down-regulated the production of TNFα in primary synoviocytes, peripheral monocytes, and murine RAW264.7 macrophages at the mRNA level. Our results also indicated that butyrate induced an ARE-binding protein, TIS11B, that could facilitate TNFα mRNA degradation. The collective data led us to believe that the down-regulation of TNFα expression by butyrate was mediated through the TIS11B protein that bound to a specific ARE and facilitated mRNA degradation.

TNFα is a key cytokine in the pathogenesis of RA. Therefore, inhibition of the action of TNFα may improve the clinical course of patients with RA. Biologic agents designed to interfere with the action of TNFα

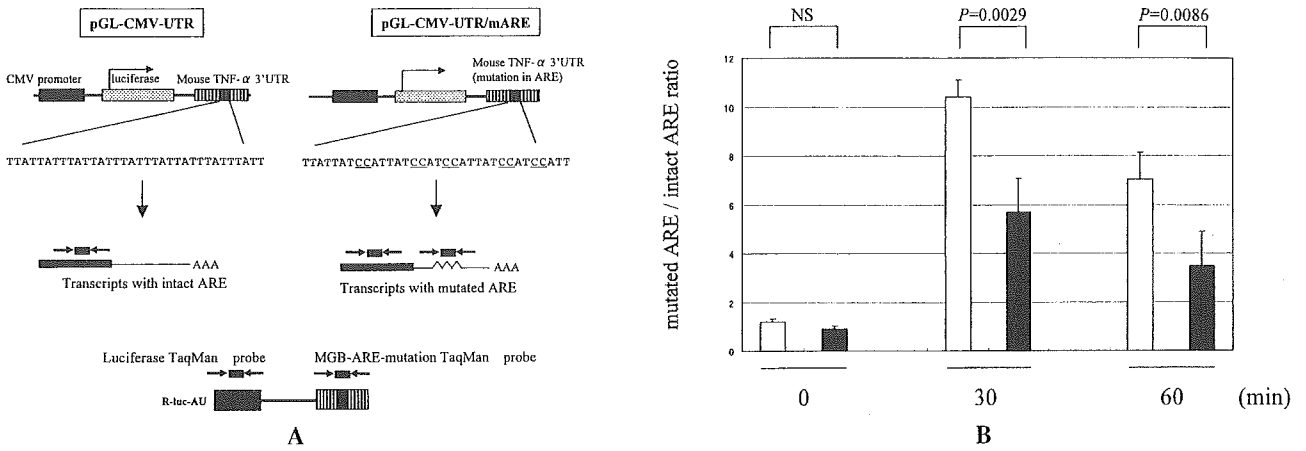


**Figure 6.** Effects of mutations in AU-rich elements (AREs) on the ability of butyrate to modify mRNA turnover. **A,** Schematic diagram of the plasmids, primers, and TaqMan probes that were used in these experiments. The plasmid pGL-CMV-UTR/mARE was derived by mutating the ARE of the 3′-untranslated region (3′-UTR) of the plasmid pGL-CMV-UTR (see Materials and Methods). To measure the gene copy number of the transcripts derived from pGL-CMV-UTR and pGL-CMV-UTR/mARE, the artificial DNA fragment R-luc-AU was generated from pGL-CMV-UTR/mARE by polymerase chain reaction (PCR) amplification. The R-luc-AU fragment, which contained both the ARE mutation and part of the common luciferase open reading frame sequence, was used to produce both the standard curve for the total luciferase transcripts and the curve for transcripts containing the ARE mutation. **B,** Quantitative PCR analysis of the reporter gene products carrying intact or mutated ARE. RAW264.7 cells were transfected with a 50:50 mixture of pGL-CMV-UTR/mARE and pGL-CMV-UTR. Cells were then not treated (solid bars) or pretreated with 5 m*M* sodium butyrate for 2 hours (open bars) and placed in culture medium containing actinomycin D (10 μg/ml) to halt transcription. Cells were then harvested serially at 0-, 30-, and 60-minute time points, and total RNA was extracted. Degradation of plasmid DNA and subsequent cDNA synthesis were carried out using the same method described in Figure 5. Real-time quantitative PCR analyses were done using a TaqMan probe, with specific forward and reverse primers (see Materials and Methods). The amounts of total luciferase cDNA transcripts and transcripts with mutated ARE were determined, and the y-axis shows the ratio of cDNA transcripts with mutated ARE to cDNA transcripts with intact ARE. Data were obtained from triplicate transwells and are representative of 5 independent experiments. Values are the mean and SEM. CMV = cytomegalovirus; TNFα = tumor necrosis factor α; MGB = minor groove binder; NS = not significant.

have been approved for the treatment of RA, and they provide dramatic efficacy for the affected patients. However, the disadvantages of biologic agents, such as their high cost, their instability, the difficulty of producing them, and the immune reaction of the host toward them, remain to be addressed. Therefore, new chemical agents that down-regulate TNFα production have been researched extensively. Our current findings may provide a framework for the therapeutic down-regulation of TNFα production by butyrate or its analogs.

Butyrate facilitated the degradation of luciferase transcripts when the TNFα 3′-UTR cDNA sequence was included in the reporter construct. This effect appeared to be dependent on an ARE, since a mutation in the ARE in the reporter plasmids resulted in the loss of the butyrate-induced changes in the transcript turnover. Thus, butyrate could down-regulate TNFα mRNA expression by facilitating TNFα mRNA degradation through a mechanism that was dependent on the specific ARE.

AREs are several repetitive sequences of AUUUA or UUAUUUAUU present in the 3′-UTRs of various mRNA. The AREs are clustered into several categories and have been identified in a panel of genes other than TNFα (27–30). These genes largely encode proteins that regulate cellular growth and the body's response to exogenous agents such as microbes and inflammatory and environmental stimuli. The mRNA containing AREs are commonly short lived, rapidly expressed in response to stimuli, and rapidly degraded once their critical role in gene regulation ceases.

To date, several ARE-binding proteins have been reported that can stabilize or destabilize the target mRNA by binding competitively to their AREs. TTP (also known as TIS11, Nup475, and G0S24) is one of these ARE-binding proteins, and it has been characterized as a critical factor that controls TNFα mRNA turnover (31). Interestingly, genetically manipulated mice that lack TTP showed an abundance of endogenous TNFα production, an RA-like arthritis, and autoimmunity, presumably mediated by an excess of TNFα (32–34). TTP-related proteins, designated TIS11B and TIS11D, are structurally similar to TTP in their zinc-finger motifs, and they share functions with TTP, al-